Unraveling the forcings controlling the vegetation and climate of the best orbital analogues for the present interglacial in SW Europe

Dulce Oliveira, Stéphanie Desprat, Qiuzhen Yin, Filipa Naughton, Ricardo Trigo, Teresa Rodrigues, Fátima Abrantes & Maria Fernanda Sán

Climate Dynamics
Observational, Theoretical and Computational Research on the Climate System

ISSN 0930-7575

Clim Dyn
DOI 10.1007/s00382-017-3948-7

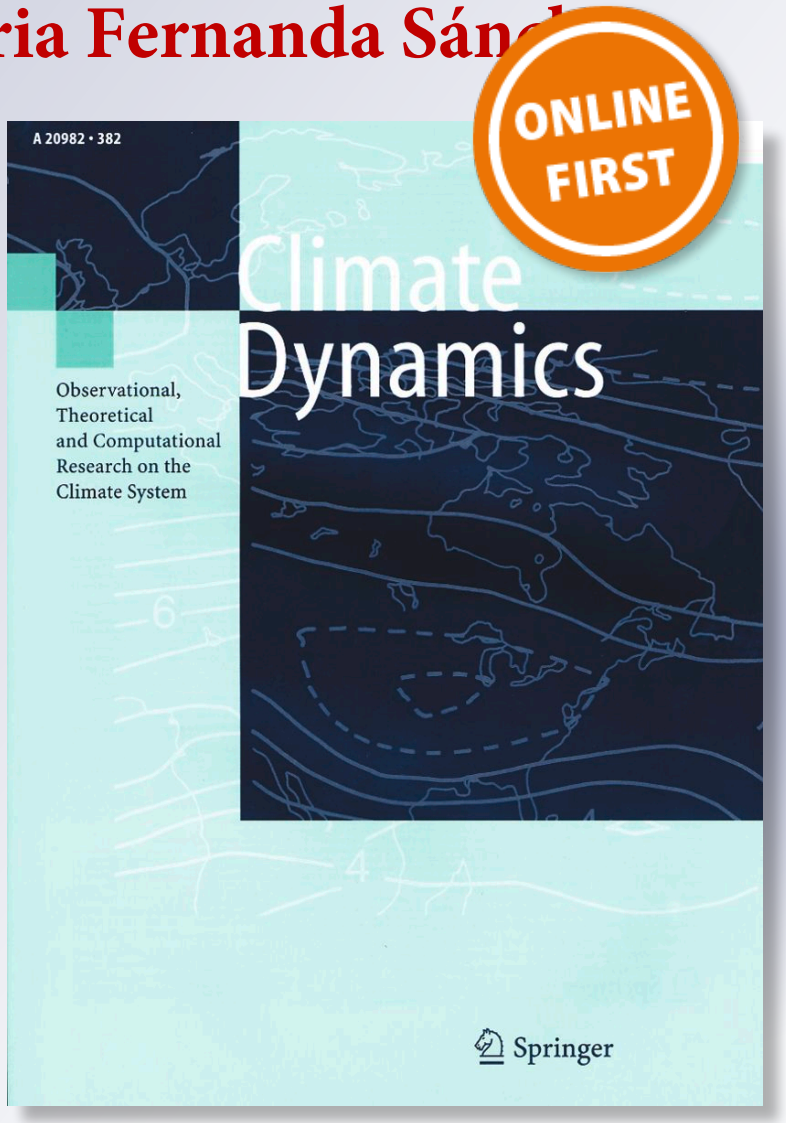

Springer

Clim Dyn
DOI 10.1007/s00382-017-3948-7

Unraveling the forcings controlling the vegetation and climate of the best orbital analogues for the present interglacial in SW Europe

Dulce Oliveira[1,2,3,4] · Stéphanie Desprat[1,2] · Qiuzhen Yin[5] · Filipa Naughton[3,4] · Ricardo Trigo[6] · Teresa Rodrigues[3,4] · Fátima Abrantes[3,4] · Maria Fernanda Sánchez Goñi[1,2]

Received: 17 March 2017 / Accepted: 30 September 2017

Abstract The suitability of MIS 11c and MIS 19c as analogues of our present interglacial and its natural evolution is still debated. Here we examine the regional expression of the Holocene and its orbital analogues over SW Iberia using a model–data comparison approach. Regional tree fraction and climate based on snapshot and transient experiments using the LOVECLIM model are evaluated against the terrestrial–marine profiles from Site U1385 documenting the regional vegetation and climatic changes. The pollen-based reconstructions show a larger forest optimum during the Holocene compared to MIS 11c and MIS 19c, putting into question their analogy in SW Europe. Pollen-based and model results indicate reduced MIS 11c forest cover compared to the Holocene primarily driven by lower winter precipitation, which is critical for Mediterranean forest development. Decreased precipitation was possibly induced by the amplified MIS 11c latitudinal insolation and temperature gradient that shifted the westerlies northwards. In contrast, the reconstructed lower forest optimum at MIS 19c is not reproduced by the simulations probably due to the lack of Eurasian ice sheets and its related feedbacks in the model. Transient experiments with time-varying insolation and CO_2 reveal that the SW Iberian forest dynamics over the interglacials are mostly coupled to changes in winter precipitation mainly controlled by precession, CO_2 playing a negligible role. Model simulations reproduce the observed persistent vegetation changes at millennial time scales in SW Iberia and the strong forest reductions marking the end of the interglacial "optimum".

Keywords Orbital Holocene analogues · Model–data comparison · Mediterranean vegetation · Marine pollen analysis · Insolation · CO_2

Electronic supplementary material The online version of this article (doi:10.1007/s00382-017-3948-7) contains supplementary material, which is available to authorized users.

✉ Dulce Oliveira
dulce.oliveira@ipma.pt

1 EPHE, PSL Research University, 33615 Pessac, France

2 Laboratoire Paléoclimatologie et Paléoenvironnements Marins, University of Bordeaux, EPOC, UMR 5805, 33615 Pessac, France

3 Divisão de Geologia e Georecursos Marinhos, Instituto Português do Mar e da Atmosfera (IPMA), Avenida de Brasília 6, 1449-006 Lisboa, Portugal

4 CCMAR, Centro de Ciências do Mar, Universidade do Algarve, Campus de Gambelas, 8005-139 Faro, Portugal

5 Georges Lemaître Center for Earth and Climate Research, Earth and Life Institute, Université catholique de Louvain, Louvain-la-Neuve, Belgium

6 Instituto Dom Luiz, Universidade de Lisboa, 1749-016 Lisboa, Portugal

1 Introduction

Past warm intervals are critical experiments for testing how the natural climate system responds to different forcing factors under reduced ice sheets compared to glacial periods. Two Quaternary interglacials, the Marine Isotope Stage (MIS) 11 (425–374 ka; MIS 11c, 425–395 ka) and MIS 19 (790–761 ka; MIS 19c, 790–774 ka), have received particular attention from the scientific community owing to their relatively similar orbital characteristics with the Holocene (e.g. Berger and Loutre 2002, 2003; Tzedakis et al. 2012; Candy et al. 2014). Such analogy is based on akin low eccentricity and weak precession variations, albeit when the summer half-year insolation is considered both interglacials appear less analogous to MIS 1 (Tzedakis et al.

Published online: 20 October 2017

2017). MIS 11c has long been considered the most appropriate astronomical analogue for the Holocene and its climatic progression since it displays a similar seasonal and latitudinal distribution of insolation, which is largely responsible for the climatic structure and duration of interglacials (e.g. Droxler and Farrell 2000; Berger and Loutre 2002, 2003; Loutre and Berger 2003; Candy et al. 2014). Based on this similarity, the current interglacial was predicted to be exceptionally long, lasting for more 50,000 years (Berger and Loutre 2002). However, MIS 11c orbital analogy with the Holocene and its future remains complex and controversial mainly due to the uncertainties in the precise alignment of the two interglacials (e.g. EPICA 2004; Ruddiman 2005; Masson-Delmotte et al. 2006; Tzedakis 2010) and the seemingly contradictory evidence in both the climatic structure and greenhouse gas (GHG) concentrations (e.g. Bauch et al. 2000; McManus et al. 2003; de Abreu et al. 2005; Ruddiman 2007; Helmke et al. 2008; Dickson et al. 2009; Pol et al. 2011; Kandiano et al. 2012; Melles et al. 2012; Candy et al. 2014; Ganopolski et al. 2016). Regardless of MIS 11c suitability as an orbital analogue of the Holocene, this interglacial presents additional key features, including its higher than present sea-level probably associated to the collapse of Greenland and West Antarctica ice sheets (e.g. de Vernal and Hillaire-Marcel 2008; Raymo and Mitrovica 2012; Roberts et al. 2012; Reyes et al. 2014; Dutton et al. 2015) and its GHG-driven climate warming (Raynaud et al. 2005; Yin and Berger 2012). MIS 19c phasing between precession and obliquity is more similar to MIS 1 than MIS 11c, a reason why it has been suggested as an even better analogue for the Holocene in terms of orbital configuration, insolation distribution pattern and paleoclimatic signatures (Tzedakis et al. 2009a, 2012; Pol et al. 2010; Rohling et al. 2010; Tzedakis 2010; Yin and Berger 2012, 2015; Giaccio et al. 2015). Considering MIS 19c as an analogue and assuming that ice growth mainly responds to insolation and CO_2 forcing, with [CO_2] maxima of 240 ppmv, Tzedakis et al. (2012) propose 1500 additional years to the current interglacial. However, recent work also challenges this analogy based on the different millennial-scale climatic cyclicity observed throughout the two interglacials that appears to interact with the orbital variability in triggering glacial inception (Sánchez Goñi et al. 2016).

Yin and Berger (2012, 2015) have evaluated, using the LOVECLIM model, the individual contributions of the primary forcings (insolation and GHG) to the variability of distinct climate-related parameters (temperature, tree fraction, sea ice) of the interglacials. Their analysis focused at the interglacial climate "optimum" but also over the entire periods of each interglacial. Those authors found that MIS 11c and MIS 19c can be considered as the best analogues, particularly MIS 19c, for the present interglacial from an astronomical point of view and as far as annual and seasonal temperatures under the combined effect of the primary forcings are concerned (Yin and Berger 2012, 2015). The major difference of MIS 11c would be related to its higher GHG-driven warming that results in a warmer interglacial than MIS 1 and MIS 19c (Yin and Berger 2012, 2015). As highlighted by Yin and Berger (2015), looking for analogues implies the intercomparison of the interglacials not only at the global scale but also at the regional scale. The regional expression of these past interglacials remains, however, poorly documented due to the scarcity of proxy data and model experiments. This study aims at filling this gap for the western Mediterranean region by comparing new and published terrestrial and marine climate profiles of MIS 1 (this work) to MIS 11c (Oliveira et al. 2016) and MIS 19c (Sánchez Goñi et al. 2016) from IODP Site U1385. This site covers the last 1.45 Ma and is located on the SW Iberian margin, a region particularly sensitive to climate change and the effect of precession (Ruddiman and McIntyre 1984). Based on proxy records and model simulations, here we examine the regional expression of the three interglacials, MIS 1, MIS 11c and MIS 19c, marked by low eccentricity to identify the controlling factors responsible for the magnitude and evolution of the western Mediterranean tree fraction and climate.

2 Modern setting

IODP Site U1385 (37°34.285′N, 10°7.562′W; 2578 m water depth) was recovered on the SW Iberian margin (Fig. 1), located on the eastern edge of the North Atlantic subtropical gyre (Expedition 339 Scientists 2013; Hodell et al. 2013). The modern surface hydrography off western Iberia is mainly influenced by the Portugal Current and the Azores Current, depending on the meridional displacements of the subtropical Azores High and the large-scale wind regimes (Fiúza 1984; Peliz et al. 2005). During the summer, the climate of southern Iberia is directly affected by the northeastward expansion of the Azores High, while the dynamics of the North Atlantic westerlies dominate in wintertime (Trigo et al. 2004; Lionello et al. 2006). These complex atmospheric interactions result in the high-seasonality of the Mediterranean climate (warm/dry summers and mild/wet winters), which promotes the development of a Mediterranean vegetation in SW Iberia (Castro et al. 1997). As shown by Naughton et al. (2007), the pollen signature from the SW Iberian deep-sea sediments reflects the regional vegetation of the adjacent landmasses, in particular the vegetation colonizing the hydrographic basins of the Tagus and Sado rivers. Because the vegetation distribution of these basins is closely related to precipitation and thermal gradients, conifers (*Pinus* woodland with *Juniperus)* generally dominate the highest elevations and deciduous oak the mid-altitude

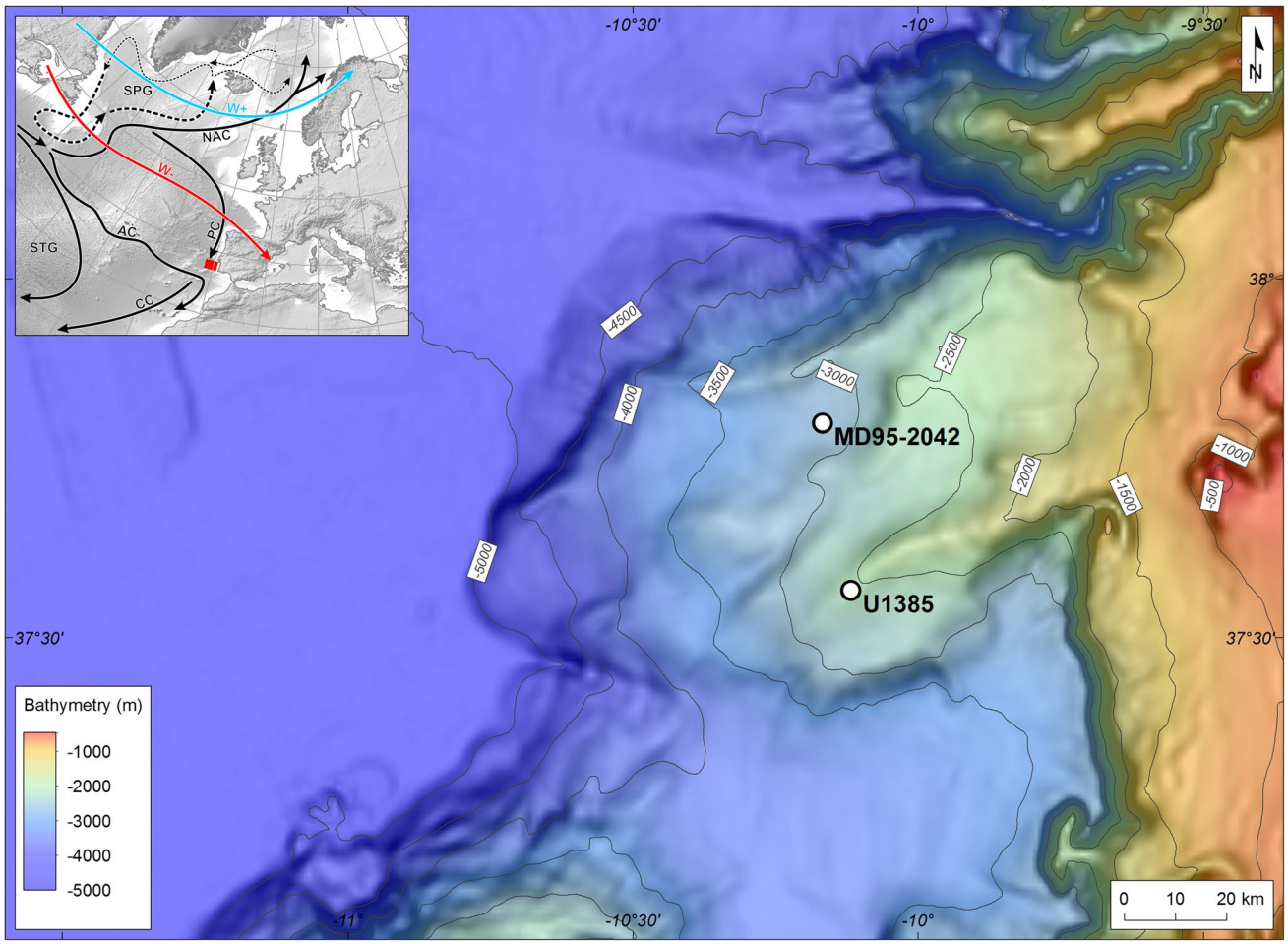

Fig. 1 Map of the SW Iberian margin showing the detailed bathymetry and location of Site U1385 and the core MD95-2042. Left inset: General geographical map showing the Iberian Peninsula. The zonal (red arrow) and meridional (blue arrow) trajectory the atmospheric westerlies is shown. Black arrows represent the surface water circulation (*SPG* Subpolar Gyre, *NAC* North Atlantic Current, *AC* Azores Current, *STG* Subtropical Gyre, *CC* Canary Current, *PC* Portugal Current)

areas (Peinado Lorca and Martínez-Parras 1987; Castro et al. 1997). Evergreen oak and Mediterranean sclerophylls (*Olea sylvestris, Pistacia lentiscus, Phillyrea*) occupy the warmest zones at lower elevations (Castro et al. 1997). Heathlands (Ericaceae) are naturally confined to zones with relatively high humidity and rockrose shrublands (Cistaceae) expand in drier environments (Peinado Lorca and Martínez-Parras 1987; Loidi et al. 2007).

3 Materials and methods

3.1 Chronology

MIS 1 chronology was established from five AMS radiocarbon dates converted to calendar year before present (cal yr BP) using the Marine13 curve (Reimer et al. 2013) with Calib 7.1 (Stuiver and Reimer 1993; http://calib.qub.ac.uk/calib/) (Fig. 2; Table S1). The lower part of the age-depth model was constrained by one additional control point from the age model "Age_Depth_Radiocarbon" of Hodell et al. (2015) that is based on correlating the Ca/Ti record of Site U1385 to the $CaCO_3$ record of the nearby MD99-2334 core, which has a robust radiocarbon chronology (Fig. 2). The age-depth model was obtained using linear interpolation between each of the six control points (Fig. 2). The studied core section encompasses the last 17.5 ka and the average temporal resolution for the pollen and SST record is ~ 465 year (Fig. 3). MIS 11c and MIS 19c paleoclimate records are presented on their original LR04-derived chronology (Hodell et al. 2015; Oliveira et al. 2016; Sánchez Goñi et al. 2016) with an average temporal resolution of ~ 475 year (Fig. 4).

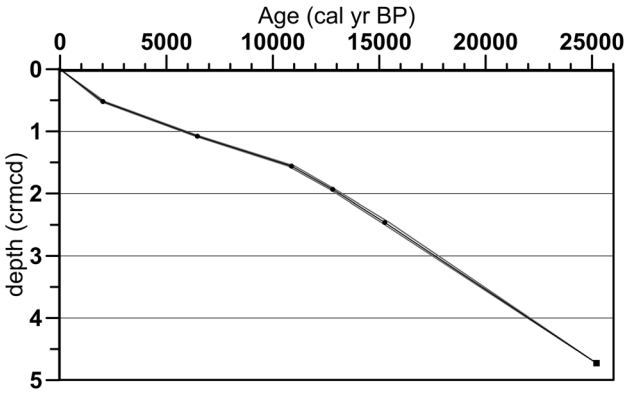

Fig. 2 Age–depth model based on five calibrated AMS radiocarbon ages (black circles, Table S1) and one control point from the radiocarbon age model of Site U1385 (black square, Hodell et al. 2015). Grey lines indicate the 2σ uncertainty envelope

3.2 Pollen and alkenones analyses

Five Holes (A–E) were drilled at Site U1385 using an advanced piston corer system during the IODP Expedition 339 (Mediterranean Outflow) (Fig. 1) (Hodell et al. 2013). Correlation among Holes was performed based on X-ray fluorescence core scanning at 1-cm resolution, which allowed the construction of a continuous spliced stratigraphic section spanning the last 1.45 Ma (Hodell et al. 2015).

Thirty-eight levels were sampled from Holes E and D every 5 to 10 cm between 0.05 and 2.92 corrected revised meter composite depth (crmcd). The new pollen and biomarkers analyses followed the methodology described by Oliveira et al. (2016) and Sánchez Goñi et al. (2016) for the study of MIS 11c and MIS 19c. Pollen samples were processed using the standard protocol for marine samples including coarse-sieving (150 µm mesh), treatment with cold HCl and cold HF, microsieving (10 µm mesh) and slide preparation in glycerol (http://ephe-paleoclimat.com/ephe/Pollen%20sample%20preparation.htm). A minimum of 20 pollen morphotypes and 100 pollen grains excluding *Pinus, Cedrus*, aquatics and Pteridophyta spores were counted in each sample. Pollen percentages were calculated based on the main pollen sum excluding *Pinus* due to its well-known over-representation in marine sediments (e.g. Heusser and Balsam 1977), including those from the western Iberian margin (Naughton et al. 2007). Also excluded were *Cedrus*, because it is an exotic pollen grain that likely originates from the North African cedar forest (Magri 2012), aquatic plants, spores and indeterminable pollen grains. The Mediterranean forest (MF) pollen percentage record comprises the Mediterranean taxa and all temperate tree and shrub taxa excluding *Pinus, Cedrus* and Cupressaceae. Alkenone-based sea surface temperature ($U^{k'}_{37}$-SST) reconstruction was based on the proportion of long chain di- and tri- unsaturated C_{37} alkenones. Alkenones sediment extraction procedure followed Villanueva et al. (1997). $U^{k'}_{37}$-SST was estimated using the $U^{k'}_{37}$ index (Prahl and Wakeham 1987) and the global core-top calibration of annual SST (Müller et al. 1998).

3.3 Model and experimental setup

The climate model experiments were performed with the LOVECLIM three-dimensional Earth system model of intermediate complexity (Goosse et al. 2010). In these simulations, the atmospheric component (ECBilt), sea-ice-ocean model (CLIO) and terrestrial biosphere (Vegetation COntinuous Description—VECODE) were interactively coupled while the carbon cycle and the ice sheets were fixed to their present-day values (Yin and Berger 2012, 2015). VECODE is a model of reduced complexity in which the vegetation dynamics, defined as a fractional distribution of desert, tree and grassland, are simulated as a non-linear function of the climatic conditions, in particular the accumulation of daily positive degrees during the year, i.e. the growing degree-days above 0 °C (GDD0), and the annual mean precipitation (Brovkin et al. 1997). An extensive description of the model and experiment design used in this study is provided in Yin and Berger (2012, 2015).

The climate "optimum" of each interglacial was simulated with two sets of snapshot experiments using the astronomical parameters (1) at times when Northern Hemisphere summer occurs at perihelion (NHSP) (12, 409 and 788 ka) and (2) at the interglacial benthic $\delta^{18}O$ peaks of the LR04 stack from Lisiecki and Raymo (2005) (6, 405 and 780 ka) (Yin and Berger 2015). The peak interglacial GHG concentrations were used in the simulations and ice sheets were prescribed to their present-day configuration. The model has been integrated for 1000-year. This produced an equilibrium climate state at the end of the simulations and the last 100-year climatology was investigated. Comparison between proxy data and model results of transient experiments covering at least one precessional cycle (Yin and Berger 2015) was also carried out to investigate the regional vegetation and climate dynamics under the varying astronomical configurations and CO_2 concentrations of MIS 1 (last 15 ka), MIS 11c (425–394 ka) and MIS 19c (793–773 ka). The ice sheets were prescribed to their Pre-Industrial (PI) extent. In these simulations, an acceleration factor of 10 was used (Yin and Berger 2015).

4 Results and discussion

4.1 Direct land-sea comparison for MIS 1

The new direct land-sea comparison from Site U1385 identifies the last 17.5 ka climatic periods, well-documented in the SW Iberian terrestrial and marine

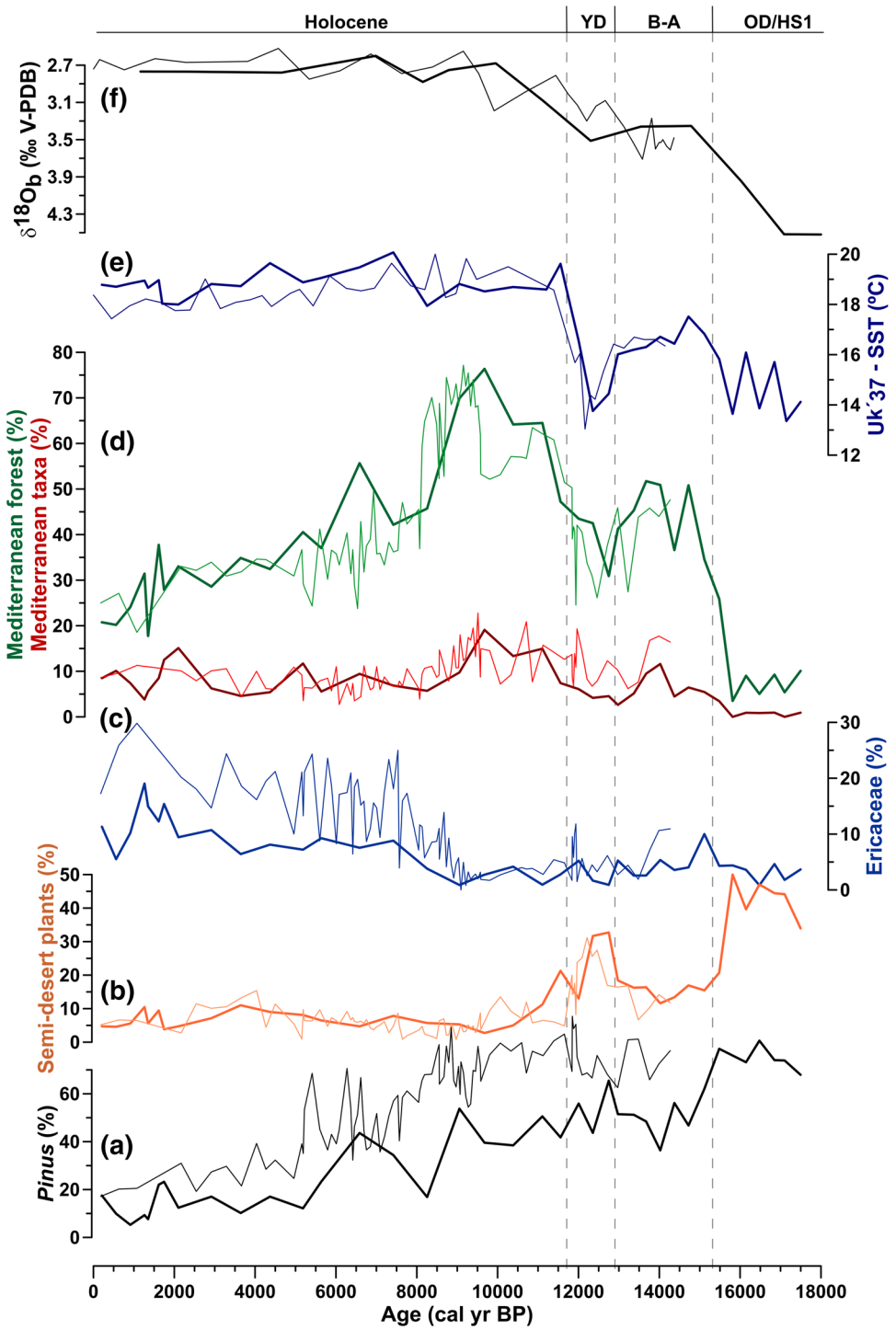

Fig. 3 Vegetation and climatic changes from Site U1385 (bold lines) and the nearby marine core MD95-2042 (thin lines) over the last 17.5 ka. From bottom to top: Percentages of selected pollen taxa or group of taxa (U1385: this study; MD95-2042: Chabaud et al. 2014): **a** *Pinus* (black), **b** semi-desert plants (*Artemisia*, Chenopodiaceae, *Ephedra distachya*-type and *Ephedra fragilis*-type) (orange), **c** Ericaceae (blue), **d** Mediterranean taxa (*Quercus evergreen*-type, *Cistus, Olea, Phillyrea* and *Pistacia*) (red) and MF (mainly deciduous *Quercus* and Mediterranean taxa) (green); **e** Uk'_{37}-SST (dark blue) (U1385: this study; MD95-2042: Pailler and Bard 2002); **f** $\delta^{18}O_b$ records (black) (U1385: Hodell et al. 2015; MD95-2042: Shackleton et al. 2000). Upper bar indicates the North Atlantic climatic phases: Oldest Dryas (OD)/Heinrich Stadial 1 (HS1), Bølling-Allerød (B-A) interstadial, Younger Dryas (YD) stadial and the Holocene interglacial

environments (e.g. Bard et al. 2000; Rodrigues et al. 2009; Chabaud et al. 2014; Salgueiro et al. 2014; Naughton et al. 2016): (1) the cold/dry Oldest Dryas (OD)/Heinrich Stadial 1; (2) the temperate/humid Bølling-Allerød (B-A); (3) the cool/relatively dry Younger Dryas (YD); and (4) the warm/humid Holocene marked by a major expansion of the MF between ~ 11.6 and 8.5 ka, followed by a progressive contraction toward the late Holocene (Fig. 3, for pollen percentage diagram and summary description see Fig. S1 and Table S2). The comparison of the pollen records from Site U1385 and the nearby core MD95-2042 (Chabaud et al. 2014) during the overlapping time interval, i.e. the last 14.2 ka, shows clear evidence for the replicability of the pollen analysis in the SW Iberian margin (Fig. 3), which is a prime location for undertake land–sea comparisons. Although the two

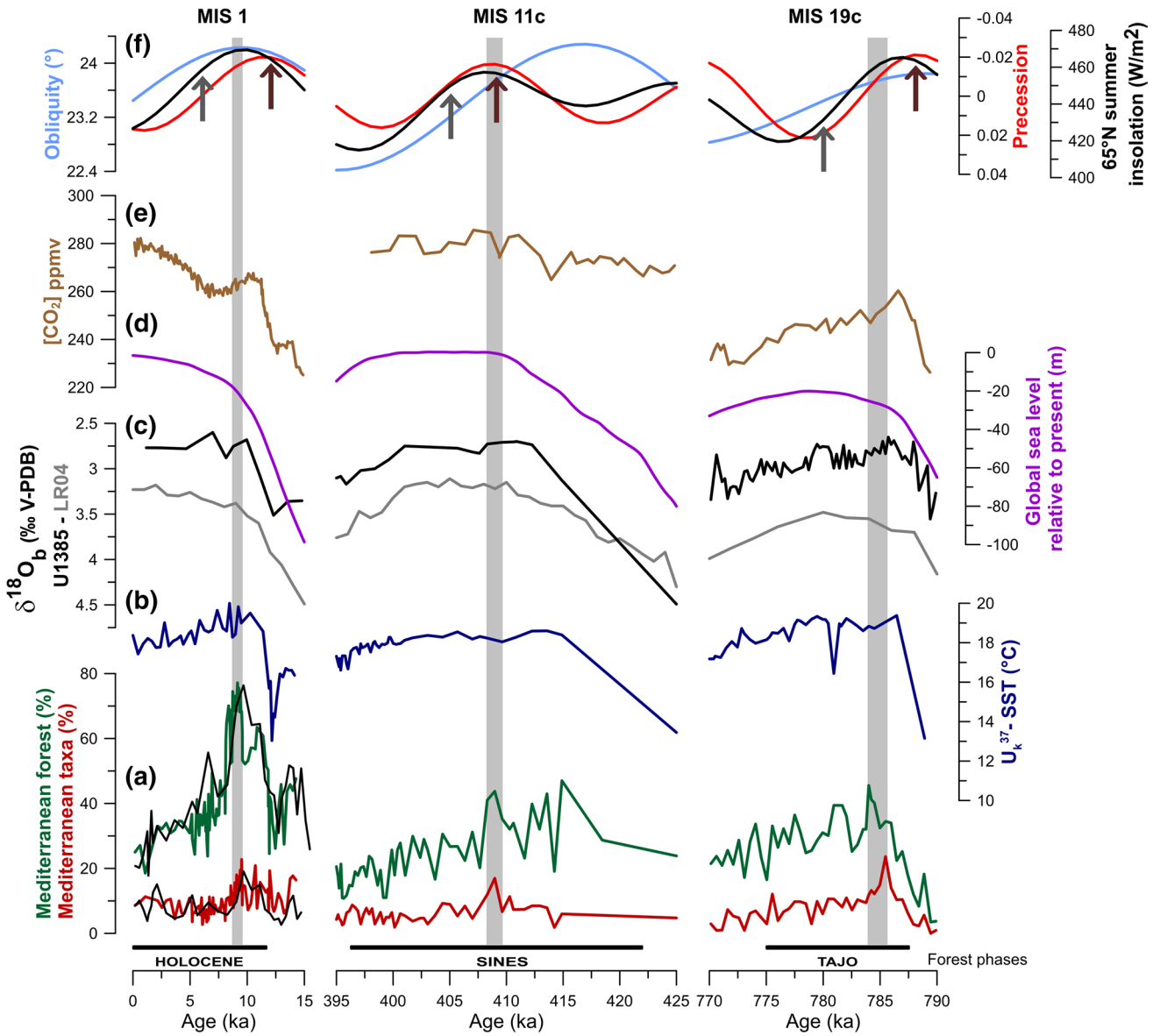

Fig. 4 Vegetation and climatic changes from Site U1385 over MIS 1, MIS 11c (Oliveira et al. 2016) and MIS 19c (Sánchez Goñi et al. 2016). From bottom to top: Selected pollen percentage curves: **a** Mediterranean taxa (MIS 1: red, Chabaud et al. 2014; black, this study) and MF (MIS 1: green, Chabaud et al. 2014; black, this study); **b** Uk'_{37}-SST (MIS 1: Pailler and Bard 2002) (dark blue); **c** $\delta^{18}O_b$ records of Site U1385 (black) (Hodell et al. 2015) and LR04 (grey) (Lisiecki and Raymo 2005); **d** Modeled global sea level relative to present (m) (purple) (Bintanja and van de Wal 2008); **e** CO_2 concentration (brown) (Lüthi et al. 2008); **f** 65°N summer insolation (black), obliquity (light blue) and precession (red) parameters (Berger 1978). The grey bars mark the interglacial vegetation "optimum", which for the Holocene was based on the MD95-2042 dataset. Arrows indicate the insolation used in the snapshot simulations at the dates when boreal summer occurred at perihelion (NHSP) (dark red) and at the dates of the LR04 $\delta^{18}O_b$ peaks (grey) (Yin and Berger 2015). Forest phases labeled with local names (bottom) and stratigraphical framework (top) are indicated

pollen diagrams diverge in the values of some taxa such as *Pinus* and Ericaceae, they bear strong similarities in terms of vegetation dynamics within the chronological uncertainties and in particular, they present similar Holocene maximal values of Mediterranean taxa and forest (Fig. 3; Table S3). Since the results of the marine proxy analyses are also in good agreement (Fig. 3) and the chronology from core MD95-2042 is more accurate (twice as many radiocarbon dates than Site U1385), hereafter we also use the higher time-resolution MD95-2042 dataset for MIS 1 (150 year average for pollen and 340 year for SST) (Figs. 3, 4, 8a, b).

4.2 Interglacial intensity in the SW Iberian region

4.2.1 Comparing reconstructed and simulated interglacial vegetation and climate "Optima" for MIS 1, 11c and 19c

The reconstructed "optimum" forest development of each interglacial in SW Iberia was determined following recent compilations that defined the interglacial intensity based on the maximum values achieved in a range of climatic proxies within the interglacials (Lang and Wolff 2011; Candy and McClymont 2013; Past Interglacials working group of PAGES 2016). Here, we started by identifying the interval with the highest percentages of Mediterranean taxa and MF (Fig. 4; Table S3) because it represents the optimal expression of the Mediterranean climate (Polunin and Walters 1985). Second, we calculated the mean pollen percentages of Mediterranean taxa and MF maxima during these intervals (Fig. 4, Table S3). Because the maximal expansion of MF and Mediterranean taxa occurred at the same date during MIS 1 and MIS 11c at Site U1385, to avoid the effect of potential outliers, the averaged interval included not only the absolute maximum value but also the values of the samples before and after it (Fig. 4; Table S3).

Site U1385 pollen record shows that MIS 1 stands out in terms of MF "optimum" development, displaying the highest MF values (72% average) (Fig. 4; Table S3). The MF maxima values of MIS 11c and MIS 19c although very similar (40 and 39% average, respectively) are substantially below the average of MIS 1 (Fig. 4; Table S3). The larger expansion of the MF during MIS 1 is mainly due to the stronger development of deciduous oak (deciduous *Quercus* pollen-type), the dominant temperate tree in the studied region that includes species with a wide range of tolerance of winter temperatures but require a rainy climate (Polunin and Walters 1985). In contrast, the Mediterranean taxa maxima values show small differences between the three interglacials (< 6%), suggesting an identical "optimum" development of these summer-drought resistant taxa (Fig. 4; Table S3) and, therefore, similar summer dryness. Interglacial sea surface conditions off SW Iberia are characterized by overall warm and relatively stable SST (Fig. 4). Nevertheless, the peak warmth of MIS 1 (maximum SST: 20 °C) is slightly higher than that of MIS 11c (18.6 °C) and MIS 19c (19.4 °C), although these differences are close to the limit of the Uk'_{37}-SST estimated uncertainty (~0.5 °C) (Villanueva et al. 1997) (Fig. 4). At the MF "optimum" development, MIS 1 SST also reached maxima ~ 1.6 and 1 °C higher than MIS 11c and MIS 19c, respectively (Fig. 4).

At present, the MF development and composition are determined not only by temperature but in particular by the moisture availability and rainfall seasonality (Quezel 2002; Gouveia et al. 2008). Given the contrasts in the vegetation composition between the three interglacials, i.e. proportion of deciduous *Quercus versus* Mediterranean taxa, and the low-amplitude variations in the $U^{k'}_{37}$-SST profiles (Fig. 4), we suggest that the different magnitude in the forest expansion was primarily driven by distinct winter precipitation conditions over the SW Iberian region. Comparison between proxy data and model results allows testing this hypothesis.

The major expansion of the SW Iberian forest during MIS 1, 11c and 19c shows closer correspondence to NH summer insolation maxima than to LR04 $\delta^{18}O_b$ peaks (Fig. 4), within age uncertainties. Therefore, it appears more appropriate to compare our pollen-based reconstructions with the snapshot simulations of the interglacial climate "optimum" in which the insolation of NHSP is used (Figs. 5, 6a, b, 7). This approach is further supported by the evidence of the pervasive influence of precession on the long-term Mediterranean vegetation patterns, with Mediterranean plants displaying maxima associated with precession minima (Magri and Tzedakis 2000). In addition, recent work (Yin and Berger 2015) comparing the results of the two sets of snapshot experiments with the proxy data of five warm interglacials, MIS 1, 5e, 9e, 11c and 19c, showed that the simulations using the insolation of NHSP provide a better agreement with the proxy reconstructions than the ones using the insolation at the interglacial $\delta^{18}O_b$ peaks.

The simulated tree fraction during MIS 1 climate "optimum" over southern Iberia was significantly higher than during MIS 11c but not significantly different from MIS 19c (Fig. 5). Assuming that the MF pollen percentages at Site U1385 represent the SW Iberian tree fraction, both pollen-based vegetation records and snapshot experiments agree on reduced MIS 11c forest cover compared to MIS 1, however, the model is not able to reproduce the differences between MIS 19c and MIS 1 (Figs. 4, 5). The modeled tree fraction using transient simulations, which provide a broader view of the vegetation response to a time-varying forcing (insolation and GHG), further shows that the tree fraction peaks of MIS 1 and MIS 19c are similar and larger than MIS 11c (Fig. 8a, b). However, one should keep in mind that the relationship between arboreal pollen percentages and tree cover is not direct, which is mostly due to the difficulty of estimating the role of all the different factors influencing the palynological data (e.g. pollen productivity and dispersability, source area and distance to sample site, amenability to wind dispersal, deposition and preservation until sampling and analysis of vegetation dynamics) (Bradshaw and Webb 1985; Prentice et al. 1987; Faegri et al. 1989). Nevertheless, this does not affect our pollen-vegetation relationships as previous work has shown that the pollen percentage variations reflect the past tree cover patterns (Williams and Jackson 2003) and vegetation composition (Nieto-Lugilde et al. 2015). In addition, although the vegetation model VECODE has shown to yield results that agree fairly well with more complex

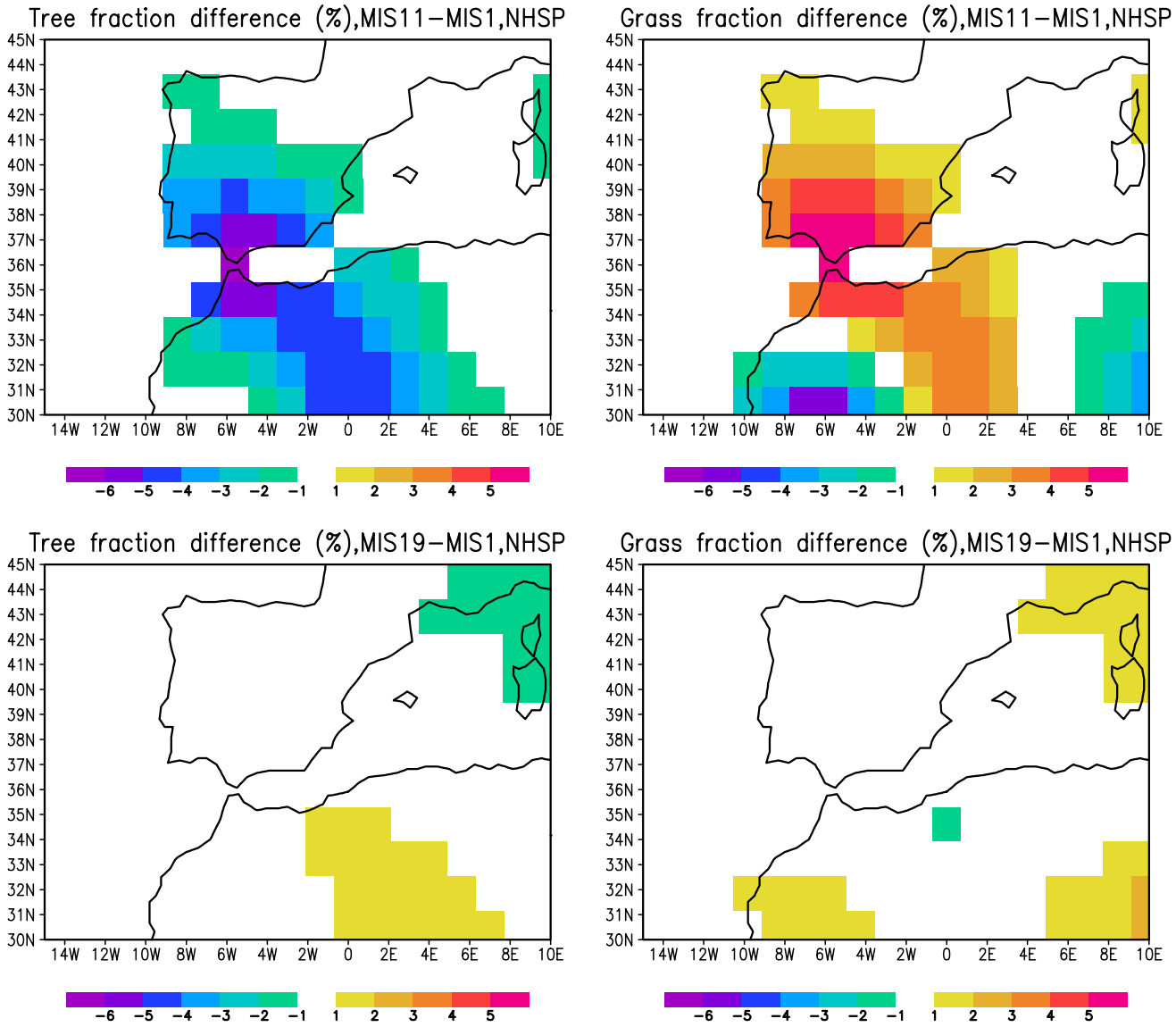

Fig. 5 Differences between MIS 1 and MIS 11c (upper panel) and MIS 19c (lower panel) for the tree and grass fraction change (%) using the snapshot simulations with insolation of NHSP

vegetation models and observations (Cramer et al. 2001), the simplicity of this model also precludes a quantitative comparison between the simulated and reconstructed regional tree fraction and a quantitative analysis of the simulated differences in the climate parameters. VECODE simulates the percentage of tree fraction only as a function of GDD0 and annual mean precipitation (Brovkin et al. 1997), neglecting the importance of the seasonality of the Mediterranean climate in driving vegetation changes in SW Iberia. Simulated tree fraction can be under or overestimated without affecting qualitatively the model results. Both the uncertainties in the quantitative pollen-based reconstructions and the lack of seasonal forcing in the model outputs hamper a model-data quantitative comparison and may explain the marked differences between the values of the pollen-based and simulated tree fraction (Figs. 4, 5, 8a, b).

The simulated differences in precipitation and surface air temperature between MIS 11c and MIS 1 reveal that the modeled lower tree fraction of MIS 11c in SW Iberia is due to its relatively lower annual precipitation since the annual temperature is slightly warmer than the one of MIS 1 (Figs. 5, 6a). As the VECODE model only uses the annual mean precipitation to compute the vegetation dynamics, the influence of the seasonal distribution of precipitation in the simulated tree fraction cannot be straightforward determined. However, given the characteristic summer–dry/winter–wet character of the Mediterranean climate, the winter precipitation is the most likely main contributor to

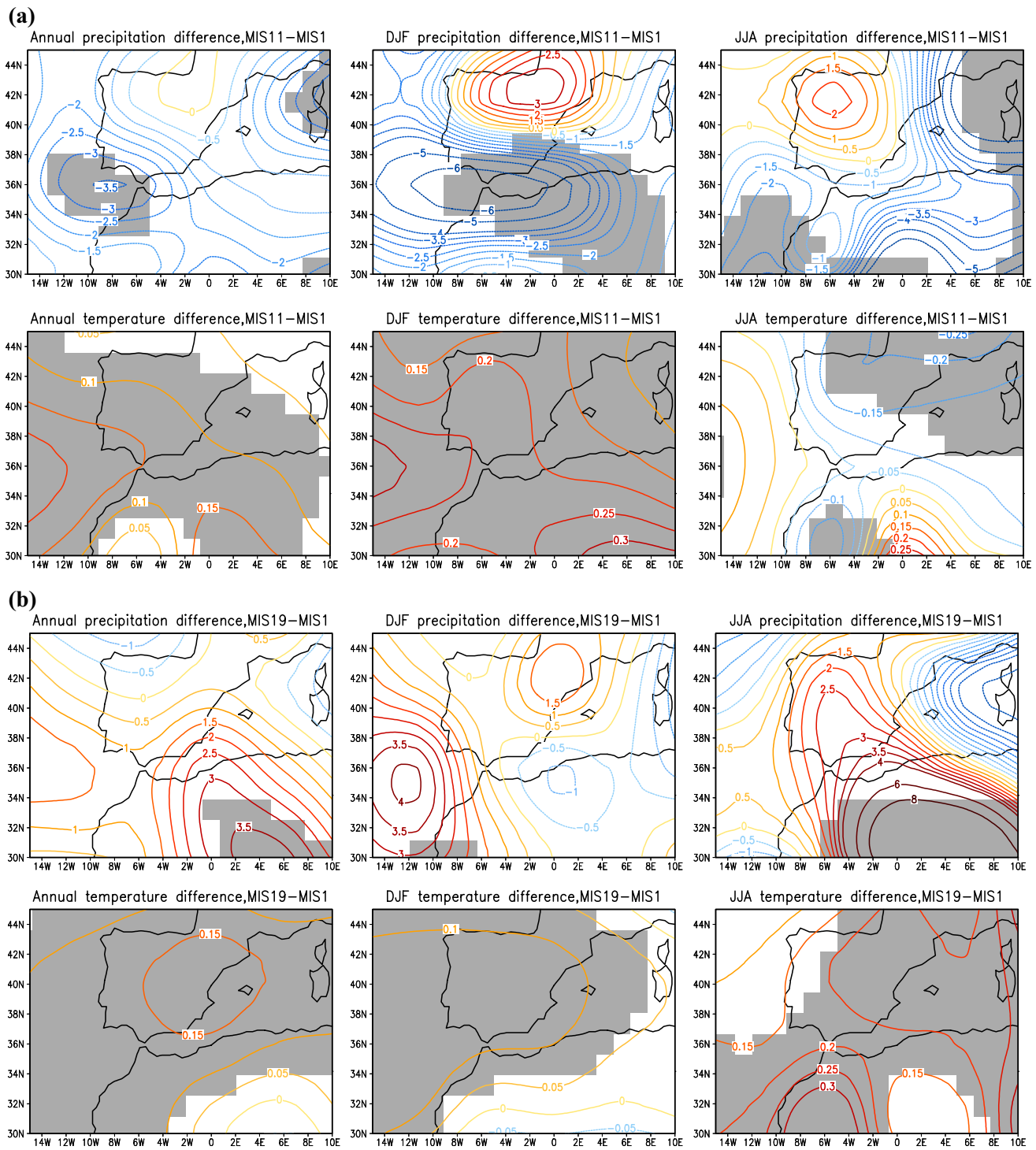

Fig. 6 **a** Differences between MIS 11c and MIS 1 using the snapshot simulations with insolation of NHSP for the annual mean, DJF and JJA precipitation (cm/year) (upper panel) and annual mean, DJF and JJA surface air temperature (°C) (lower panel). Grey shaded areas indicate the regions for which the simulated anomalies are significantly different at the 90% confidence level based on a t test. **b** Same as Fig. 6a but for the differences between MIS 19c and MIS 1

the annual mean, which is in line with the simulated lower winter (DJF) precipitation of MIS 11c, whereas the differences during the summer (JJA) are not significant (Fig. 6a). Considering the absence of differences in the simulated SW Iberian tree fraction between MIS 19c and MIS 1 (Fig. 5), as anticipated, MIS 19c annual precipitation is not significantly

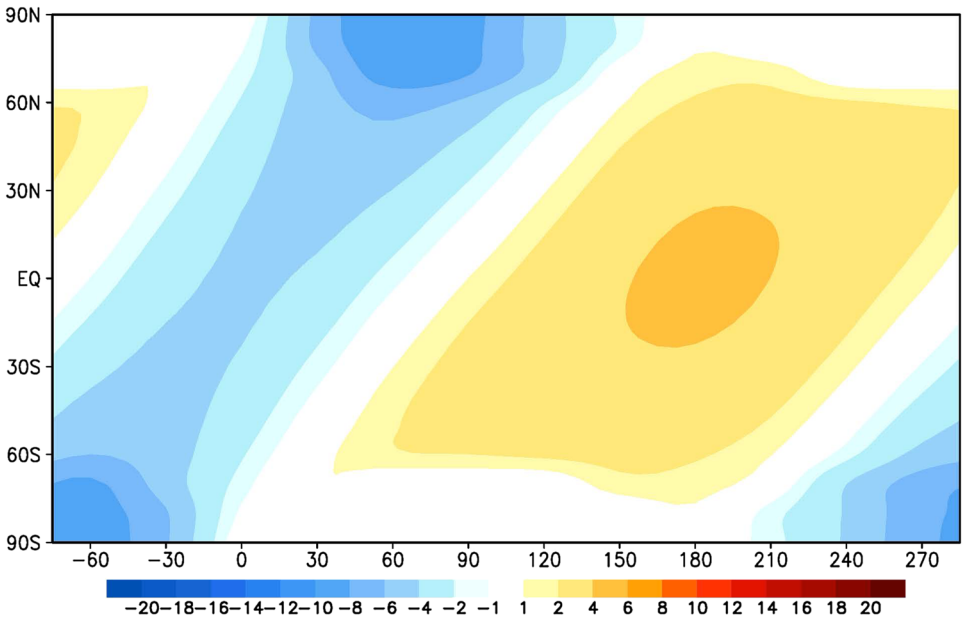

Fig. 7 Differences between MIS 11c and MIS 1 at the NHSP dates for the latitudinal and seasonal distribution of insolation (W/m^2). The Y-axis indicates latitude and the X-axis marks the true longitude of the Sun from the beginning to the end of the year (0° and 180° are for the spring and fall equinoxes; 90° and 270° are for the summer and winter solstices). Insolation is determined from the insolation parameters of Berger (1978)

different from MIS 1 and the annual surface air temperature is only slightly higher during MIS 19c (Fig. 6b). Taken together, the simulated tree fraction and climate parameters differences between MIS 11c and MIS 1 (Figs. 5, 6a) are in qualitative agreement with our pollen-based tree fraction reconstructions (Fig. 4), and consistent with our hypothesis that the relatively lower winter precipitation at MIS 11c over SW Iberia was the most important factor leading to its lower tree fraction. In contrast, the pollen-based tree fraction and inferred precipitation differences between MIS 19c and MIS 1 are not reflected in the model results (Figs. 5, 6b).

4.2.2 *What drives the SW Iberian interglacial vegetation at the climate "Optima"?*

Results of LOVECLIM simulations quantifying the insolation and GHG contribution to the tree fraction changes for the past nine interglacials showed a dominant effect of insolation on the global tree fraction change and particularly over northern tropical-subtropical regions, which was related to the strong impact of insolation (precession) on precipitation (Yin and Berger 2012). On the other hand, the CO_2 contribution only become important in the high latitudes given that the influence of temperature (GDD0) is larger than in the low latitudes (Yin and Berger 2012). Based on these findings and on the well-documented influence of precession in the Mediterranean vegetation (e.g. Magri and Tzedakis 2000; Tzedakis 2007; Sánchez Goñi et al. 2008), we consider that the major factor controlling the interglacial tree fraction maximum over SW Iberia was insolation, whereas GHG played a smaller role.

To understand the potential role of insolation and underlying mechanisms in inducing the large difference in the pollen-based tree fraction "optimum" of MIS 1 and MIS 11c over SW Iberia, we calculated the difference in the latitudinal and seasonal distribution of insolation at the NHSP dates (Fig. 6). During boreal winter, MIS 11c insolation over the high latitudes was not significantly different from MIS 1 but it was higher in the low latitudes (Fig. 6), a pattern that may have generated a larger latitudinal winter thermal gradient at the MIS 11c peak. Simulations from Yin and Berger (2012, 2015) show that MIS 11c lower obliquity led to an insolation-driven cooling at the interglacial "optimum" that was compensated by the GHG-driven warming during boreal winter, and that in the low-to-mid latitudes MIS 11c was warmer than MIS 1. This hypothesis is further supported by eastern North Atlantic SST reconstructions for MIS 1 and MIS 11c showing a steeper latitudinal temperature gradient during MIS 11c (Kandiano et al. 2012). As the latitudinal temperature gradient has a strong impact on the atmospheric circulation (e.g. Rind 1998), we propose as a working hypothesis that MIS 11c increased thermal gradient between the low and high latitudes would have led to the intensification and northward shift of the temperate westerlies with consequent decrease of winter precipitation and lower forest development over the SW Iberia region. These results are compatible with recent precipitation and circulation changes over Europe (IPCC 2013), namely with asymmetrical trends on the number of Atlantic extra-tropical cyclones and precipitation affecting northern and southern Europe (Trigo et al. 2008). Thus, while the northern Atlantic and Europe have suffered a positive trend in Atlantic mid-latitude cyclones, the Mediterranean basin is becoming drier due to fewer low-pressure systems passing through (Sousa et al. 2011). In addition, in line with recent climate model simulations for the obliquity and precession-driven changes

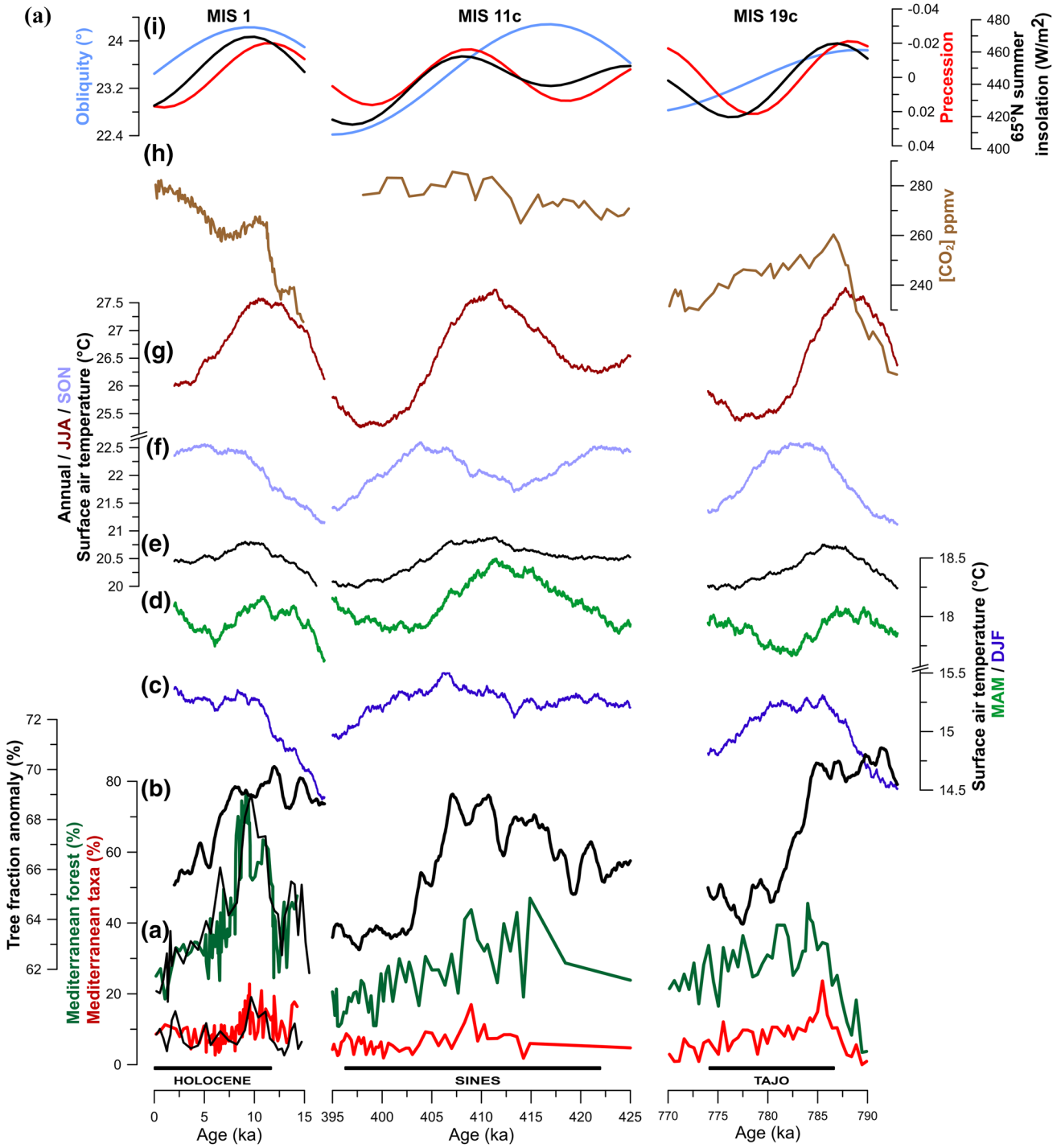

Fig. 8 **a** Vegetation and climatic changes from Site U1385 and results of the transient simulations with time-varying insolation and CO_2 for MIS 1, MIS 11c and MIS 19c for the southern Iberian region (35N°–41°N, 0–8°W). From bottom to top: Selected pollen percentage curves: *a* Mediterranean taxa (MIS 1: red, Chabaud et al. 2014; black, this study) and MF (MIS 1: green, Chabaud et al. 2014; black, this study); *b* Simulated tree fraction anomaly (%) (black); Surface air temperature (°C) *c* DJF (dark blue), *d* MAM (green), *e* annual (black), *f* SON (light blue), *g* JJA (red). The 1000-year running mean of the original simulated data is plotted. *h* CO_2 concentration (brown) (Lüthi et al. 2008); *i* 65°N summer insolation (black), obliquity (light blue) and precession (red) parameters (Berger 1978). Forest phases labeled with local names (bottom) and stratigraphical framework (top) are indicated. **b** Same as Fig. 8a but for precipitation (cm/year): *c* JJA (red), *d* annual (black), *e* MAM (green), *f* DJF (dark blue) and *g* SON (light blue)

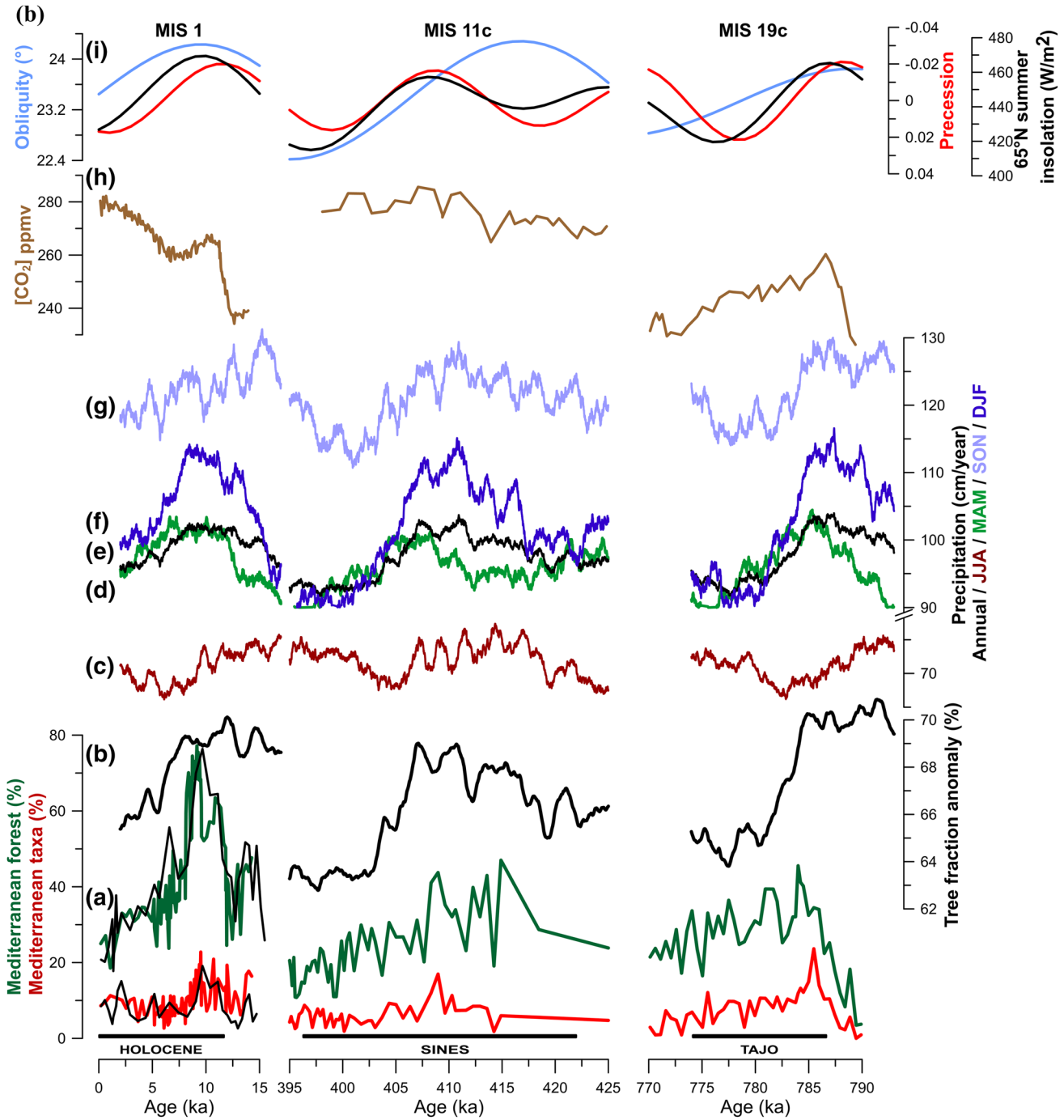

Fig. 8 (continued)

in the freshwater budget over the Mediterranean, lower obliquity and slightly lower precession minimum at the MIS 11c "optimum" may have also contributed to its lower winter precipitation by reducing the convective precipitation (Bosmans et al. 2015). These large and small-scale changes in the atmospheric circulation would explain the reduction of winter moisture availability and the resulting reconstructed and simulated lower tree fraction at the MIS 11c "optimum" in SW Iberia. However, palaeoclimate data from other key regions sensitive to the westerlies and related North Atlantic storm tracks and future simulations with more complex models are definitely needed to test our hypothesis and examine the variations in the westerlies.

The simulated tree fraction differences between MIS 1 and MIS 19c over southern Iberia show that MIS 19c is the best analogue for the Holocene "optimum" since both

snapshot and transient experiments display insignificant differences at the peak of the two interglacials (Figs. 5, 8a, b). However, pollen-based reconstructions at Site U1385 reveal a completely different pattern with much larger forest cover at the Holocene "optimum" (Fig. 4). We suggest that this model–data discrepancy mainly results from the fact that only insolation and GHG were taken into account in the simulations, thus discarding the potential impact of the different ice sheet forcing on the regional climate and vegetation. This would be particularly important for the differences between the Holocene and MIS 19c, contrasting with MIS 1 and MIS 11c during which the ice sheets in the NH were essentially restricted to Greenland (e.g. Rohling et al. 2010; Raymo and Mitrovica 2012).

According to the LR04 benthic oxygen isotope stack (Lisiecki and Raymo 2005) and marine oxygen isotope records (Hodell et al. 2008; Hodell and Channell 2016), MIS 19c ice volume was relatively higher than during the Holocene (Fig. 4). Although changes in the $\delta^{18}O$ benthic profiles are not only driven by ice volume (Skinner and Shackleton 2005), similar results have been shown by modeled global sea-level (Fig. 4) (Bintanja et al. 2005; Bintanja and van de Wal 2008) and a recent sea-level stack (Spratt and Lisiecki 2016). Proxy data and model studies evidence that prior to the Middle Pleistocene Transition (MPT, ~ 650–1100 ka) the Eurasian ice sheets had an important contribution to the total NH ice volume (e.g. Bintanja and van de Wal 2008; Hodell et al. 2008; Naafs et al. 2013). In particular, studies from the eastern North Atlantic based on organic and inorganic chemistry of ice rafted debris (IRD) demonstrate that the detrital grains of MIS 19 were not derived from the Hudson Strait but rather from northern Europe, Greenland and/or Iceland, which indicates a larger expansion of the Eurasian ice sheets in comparison to the interglacials after MIS 16 (Hodell et al. 2008; Hernández-Almeida et al. 2012; Naafs et al. 2013). We propose that these differences in ice sheet forcing between MIS 1 and MIS 19c (i.e. NH ice volume baseline conditions and Eurasian ice sheets extent) may have been responsible for the lower SW Iberian forest cover during MIS 19c and additionally explain the discrepancy between pollen-based reconstructions and climate model results. Pollen records off southern Iberia and the Mediterranean region indicate reduced forest cover for the first millennia of the early Holocene that was likely associated with the persistence of relatively large Laurentide and Fennoscandian ice sheets, which may have changed the trajectory of the mid-latitude North Atlantic storm track with consequent reduced penetration into the Mediterranean region (Magny et al. 2011, 2013; Desprat et al. 2013). In analogy to the early Holocene, we suggest that the ice sheet forcing played a major role on winter precipitation over SW Iberia, restricting the maximal forest expansion during MIS 19c. In addition, it is plausible that the volume of the Eurasian ice sheets during MIS 19c reached a significant size to increase the planetary albedo and influence the regional climate, including the SW Iberian region. Compared to MIS 1, this would have promoted regional anticyclonic conditions, i.e. relatively lower temperature and decreased humidity, with consequent lower forest cover and slightly cooler SST as suggested by our multiproxy records (Fig. 4). Such a speculation would need proper confirmation with model simulations including dynamical ice sheets accounting for example with changes in ice sheet topography and related albedo and freshwater fluxes.

Our model–data comparison strengthens previous evidence highlighting the importance for investigating the regional expression of potential past interglacial analogues for the Holocene and future climate (e.g. Lang and Wolff 2011; Candy and McClymont 2013; Yin and Berger 2015; Past Interglacials working group of PAGES 2016). Even though analogies between MIS 1, 11c and 19c have been extensively pointed out (Berger and Loutre 2002, 2003; Droxler et al. 2003; Loutre and Berger 2003; McManus et al. 2003; Tzedakis et al. 2009a, 2012; Masson-Delmotte et al. 2010; Pol et al. 2010; Tzedakis 2010; Yin and Berger 2010, 2012, 2015), our study shows that as far as the vegetation changes in SW Europe (below 40°N) are concerned, they cannot be considered as analogues for the Holocene climate "optimum". Comparison of our pollen-based reconstructions with NW Iberian margin pollen records (Desprat et al. 2007) and the long European records of Praclaux (southern France) (Reille et al. 2000; de Beaulieu et al. 2001) and Tenaghi Phillipon (NE Greece) (van der Wiel and Wijmstra 1987; Tzedakis et al. 2006) further underlines the need of looking for Holocene analogues in terms of climate and environmental impacts at the regional scale. While in the northern sites (only extending until MIS 11) where forest expansion is mainly limited by temperature, the forest "optimum" of the Holocene and MIS 11c are similar (Reille et al. 2000; de Beaulieu et al. 2001; Desprat et al. 2007), the pollen sequence from NE Greece displays the same pattern as Site U1385, showing the strongest temperate tree pollen percentages during MIS 1 and similar temperate forest expansion during MIS 11c and MIS 19c (Tzedakis et al. 2009b). It is therefore crucial to consider the key role of the hydrological changes on the interglacial vegetation and climate dynamics, particularly in regions where the vegetation communities are highly sensitive to moisture availability as the Mediterranean region (Quezel 2002).

4.3 What drives vegetation and climate variability during the Holocene and its potential analogues in SW Iberia?

To evaluate the main factors contributing to vegetation and climate variability during the entire MIS 1, 11c and 19c

in SW Iberia, we performed a comparison between pollen-based reconstructions and transient experiments with time-varying insolation and GHG. This approach allows us to overcome the problem of using a single peak forcing in the snapshot simulations and explore the major controlling factors of the vegetation changes during the different boundary conditions of each interglacial. This comparison shows that the model does not reproduce the same deglaciation vegetation change as shown by the pollen records (Fig. 8a, b). The simulated tree fraction during the deglaciations is relatively high, particularly between the last glacial-interglacial transition (B-A and YD) and the early Holocene and during the early MIS 19, which is not in agreement with the amplitude of the pollen-based vegetation changes recorded at Site U1385 (Fig. 8a, b). As changes in ice sheet forcing are one of the strongest drivers of the climate system at both global and regional scale (e.g. Clark et al. 1999; Renssen et al. 2009), we suggest that the neglected melting of the ice sheets and associated lack of ice sheet-climate interactions in our model experiments are the explanation for the large model–data discrepancies. Regrettably, this also precludes the precise identification of the onset of the maximal forest expansion in the simulations and, therefore, the model–data comparison in terms of the duration of the vegetation "optimum" interval (Fig. 8a, b). Subsequently, both pollen-based and model results show that the major expansion of the forest cover during all the three interglacials ended rapidly with a strong contraction of the forest, with no ensuing recovery to the previous degree of forest development (Fig. 8a, b). In addition, there is a good agreement between the pollen records and the modeled tree fraction over the end of each interglacial. Both pollen data and model results show that for the late part of the interglacials, the Holocene displays the highest forest extent, followed by MIS 19 while MIS 11 exhibits the lowest forest extent (Fig. 8a, b).

To determine the influence of the surface air temperature and precipitation on the vegetation changes during MIS 1, 11c and 19c, we performed simple regression analyses between the tree fraction, annual and seasonal temperature and precipitation, on the 1000-year running mean of the transient simulations original data (Fig. 8a, b; Table 1). In terms of surface air temperature (GDD0), we found that the annual mean temperature is highly correlated with the tree fraction during MIS 11c and 19c but it is not important during MIS 1, whereas in all the three interglacials the strongest correlation is obtained with JJA temperature (Fig. 8a; Table 1). As far as the precipitation is concerned, for each interglacial the tree fraction is highly correlated with the annual mean precipitation (Fig. 8b; Table 1). Because in the terrestrial biosphere model VECODE the estimation of the tree fraction does not directly involve the seasonal precipitation, the strong correlation of tree fraction with SON precipitation and particularly with DJF precipitation should be due to the high contribution of these two seasons to the annual mean precipitation (Fig. 8b; Table 1). Although the correlation analysis (Table 1) shows that the simulated tree fraction is highly correlated with summer temperature and wintertime precipitation, it is not obvious to identify from such analysis which factor is essential for vegetation change in the study region, because summer temperature and wintertime precipitation co-vary at orbital timescale since both of them are mainly controlled by precession. However, the more important role of the wintertime precipitation could be inferred from the following facts. First, the tree fraction and summer temperature curves are similar at orbital scale whereas the tree fraction and wintertime precipitation curves are similar at both orbital and millennial time scales (Fig. 8a, b). Second, the simulated (snapshot experiment) and reconstructed lower tree fraction during MIS 11c relative to MIS 1 optimum can be explained by lower winter precipitation but not by summer temperature that does not change significantly over our study region (Fig. 6a). Finally, the non-significant difference in tree fraction between MIS 19c and MIS 1 simulated by the snapshot experiments is in line with the non-significant difference in winter precipitation but not with summer temperature for which MIS 19 is significantly warmer than MIS 1 (Fig. 6b).

Table 1 Correlation coefficient values (R) of simpe linear regression between tree fraction and climate variables

	MIS 1	MIS 11c	MIS 19c
Surface air temperature			
Annual	0.10	0.94	0.70
JJA	0.85	0.94	0.94
DJF	− 0.44	0.51	− 0.28
MAM	0.24	0.76	0.41
SON	− 0.56	0.17	− 0.14
Precipitation			
Annual	0.82	0.97	0.96
JJA	0.51	0.20	0.20
DJF	0.53	0.94	0.94
MAM	0.10	0.59	0.46
SON	0.71	0.84	0.91

The calculation was made on the 1000-year running mean of the original simulated data of the transient experiments

The transient simulations under the combined effect of insolation and CO_2 indicate that the interglacial vegetation and climate dynamics over SW Iberia have no apparent relationship to atmospheric CO_2 concentration, as suggested by the pollen-based reconstructions (Fig. 8a, b). Although the direct impact of CO_2 changes on the vegetation growth is not included in the model, a prominent example for this negligible CO_2 forcing is given by its relatively high concentrations over the end of the interglacials, in particular for MIS

1 and MIS 11c, while the forest cover, annual temperature and annual precipitation achieved minimum values (Fig. 8a, b). We find that the vegetation and climate changes at this time scale are mainly driven by astronomical forcing, in particular precession, in agreement with the strong impact of precession on the climate of the Mediterranean region south of 40°N (Ruddiman and McIntyre 1984) and with previous pollen studies off southern Iberia (e.g. Fletcher and Sánchez Goñi 2008; Sánchez Goñi et al. 2008, 2016; Margari et al. 2014; Oliveira et al. 2016, 2017). As shown in Fig. 8b, in all the three interglacials the major forest expansion is concurrent with high winter precipitation, and occurs within precession minima forcing. On the contrary, low forest extent over the end of the interglacials is associated to precession maxima. These observations are in line with modeling experiments showing the dominant influence of precession in precipitation variations in subtropical regions (Yin and Berger 2012; Bounceur et al. 2015), likely driven over southern Iberia by large-scale precipitation and changes in storm track activity (Bosmans et al. 2015).

Superimposed on the vegetation changes at orbital time scale, persistent millennial-scale climate variability is revealed by a series of forest reduction events throughout the three interglacials at Site U1385 (Fig. 8a, b). Interestingly, even if a quantitative comparison in our study is not feasible, this appears to be in a good qualitative agreement with the model results. The observed intra-interglacial variability is also reproduced in the simulated tree fraction, being mainly associated to decreases in the SON and DJF precipitation (Fig. 8b) while the surface air temperatures exhibit low-amplitude and frequency variability (Fig. 8a). This leads to a view that the millennial-scale vegetation changes in SW Iberia under warm interglacial climate conditions might be essentially generated by hydrological changes primarily induced by insolation, as they are reproduced in the simulations despite the absence of ice sheet dynamics and all associated feedbacks in our experiments (Fig. 8a, b). Although further palaeoclimatic and model work is required to understand the nature of intra-interglacial variability, this study may be consistent with a growing body of evidence that outlines the importance of the low-latitude insolation forcing occurring at sub-precessional frequencies and impacting not only the low latitudes (Berger et al. 2006; Yin and Berger 2015) but also the subtropical-to-high latitudes of the North Atlantic (e.g. Weirauch et al. 2008; Ferretti et al. 2010, 2015; Billups et al. 2011; Hernández-Almeida et al. 2012; Billups and Scheinwald 2014), and in particular the SW Iberian region (Palumbo et al. 2013; Sánchez Goñi et al. 2016; Oliveira et al. 2017). On the other hand, we cannot currently exclude the hypothesis that the modeled millennial-scale vegetation changes are only caused by internal climate variability, being therefore simulated by the model with no role of orbital changes. This hypothesis should be evaluated by additional model experiments such as a multi-millennial control simulation without orbital forcing.

One of the most conspicuous features of our pollen-based reconstructions is the magnitude and the rapidity of the forest contractions marking the end of the vegetation "optimum" under prevailing interglacial warm conditions in SW Iberia, i.e. well before the substantial increase in ice volume and while SST remains high (Fig. 4). The transient simulations suggest that these changes in tree fraction might represent only a non-linear response to a gradually changing orbital forcing since in the vegetation module VECODE the relation between the tree fraction and the climatic parameters (GDD0 and annual mean precipitation) is non-linear. However, they appear more rapid in the pollen-based vegetation records than in the model simulations (Fig. 8a, b) and have previously been associated to millennial-scale variability (Chabaud et al. 2014; Sánchez Goñi et al. 2016; Oliveira et al. 2016). Therefore, we speculate that interactions between orbital and millennial-scale climate dynamics may have hastened the observed vegetation changes over the end of the interglacial optima. Additional work is required to explore the exact causes of these intriguing abrupt forest contractions recorded within full interglacial conditions.

5 Conclusions

The forcing mechanisms and regional expression of the Holocene and its best orbital interglacial analogues, MIS 11c and MIS 19c, on SW Iberia's climate and vegetation are investigated for the first time through comparison of proxy-based reconstructions and climate model experiments. This study relies on the comparison of pollen-based regional vegetation changes and alkenone-based oceanic temperature variability from IODP Site U1385, with snapshot and transient simulations that focus on the interglacial climate "optimum" and the entire interglacial periods, respectively.

1. At the interglacial climate "optimum", the pollen-based vegetation reconstructions show that the Holocene forest expansion was particularly prominent and substantially higher than at MIS 11c and MIS 19c mainly due to the stronger development of deciduous *Quercus*, which suggests higher winter precipitation. Therefore, as far as the vegetation and climatic variability in SW Europe, below 40°N, are concerned, MIS 11c and MIS 19c cannot be considered as straightforward analogues for the Holocene "optimum".

- The simulated tree fraction differences between the Holocene and MIS 11c are in qualitative agreement with the proxy evidence. As suggested by the pollen-based

reconstructions, model results show that the higher tree fraction at the Holocene "optimum" was mainly due to the greater annual mean precipitation for which the winter season was the main contributor. We propose that the amplified latitudinal insolation and thermal gradient at MIS 11c peak may have led to the northward displacement of the westerlies with consequent reduction of large-scale winter precipitation in SW Iberia, and therefore, reduced forest cover.

- In contrast to the vegetation reconstructions, in both snapshot and transient experiments MIS 19c appears to be the best analogue for the Holocene "optimum" in terms of tree fraction, with no significant differences simulated between the two interglacials in SW Iberia. These large model–data mismatches are probably related to the underestimation of the ice sheet forcing during MIS 19c as the ice sheets are kept to their Pre-Industrial values. We suggest that MIS 19c global higher ice volume and larger Eurasian ice sheets in comparison with that of the Holocene may have been responsible for its lower tree fraction, through its influence on the mid-latitude atmospheric circulation, which, in turn controls the winter hydroclimate in the Iberian Peninsula.

2. The comparison between the pollen-based and simulated interglacial vegetation with time-varying insolation and CO_2 during the entire Holocene and its potential analogues in SW Iberia reveals that the modeled tree fraction changes match the data reasonably well. A notable exception is noted for the deglaciations and attributed to the lack of ice sheet-climate interactions in the model experiments. We find that the simulated tree fraction over SW Iberia is highly correlated with warm summer temperatures and winter precipitation, with the latter being the critical factor for explaining the observed vegetation changes. On orbital time scales, our findings reveal the pervasive influence of precession on the SW Iberian forest and climate whereas no obvious relationship was found with CO_2 trends. Finally, our proxy reconstructions provide evidence for intra-interglacial instability with multiple forest decline events occurring throughout the interglacials whereas the SST remained warm off SW Iberia. Based on the transient simulations, the observed persistent millennial-scale variability during the three interglacials could result from the suborbital variation in insolation and/or internal climate variability, which should be investigated in the future. Moreover, it is remarkable that the most dramatic forest reductions ending the three interglacial "optima", during low ice volume conditions, are also reproduced in the transient experiments although they appear more gradual. This observation highlights the potential role of the interactions between orbital and millennial-scale climate dynamics in amplifying the vegetation response. Nevertheless, additional model simulations should test first if these millennial tree fraction changes represent a non-linear response to a gradual decline in insolation.

Acknowledgements Financial support was provided by WarmClim, a LEFE-INSU IMAGO project, and the Portuguese Foundation for Science and Technology (FCT) through the project CLIMHOL (PTDC/AAC-CLI/100157/2008), CCMAR (FCT Research Unit—UID/Multi/04326/2013), D. Oliveira's doctoral grant (SFRH/BD/9079/2012), F. Naughton's postdoctoral grant (SFRH/BPD/108712/2015) and T. Rodrigues's postdoctoral grant (SFRH/BPD/108600/2015). Q.Z. Yin is Research Associate of the Belgian National Fund for Scientific Research (FRS-FNRS). This research used samples provided by the Integrated Ocean Drilling Program (IODP), Expedition 339. We would like to thank the scientists and technicians of IODP Expedition 339, the Bremen Core Repository, L. Devaux for technical assistance and V. Hanquiez for drawing Fig. 1. Computational resources have been provided by the supercomputing facilities of the Université catholique de Louvain (CISM/UCL) and the Consortium des Equipements de Calcul Intensif en Fédération Wallonie Bruxelles (CECI) funded by FRS-FNRS. We thank three anonymous reviewers for their constructive and insightful comments.

References

Bard E, Rostek F, Turon J-L, Gendreau S (2000) Hydrological impact of Heinrich events in the subtropical Northeast Atlantic. Science 289:1321–1324. doi:10.1126/science.289.5483.1321

Bauch HA, Erienkeuser H, Helkme JP, Struck U (2000) A palaeoclimatic evaluation of marine oxygen isotope stage 11 in the high-northern Atlantic (Nordic Seas). Glob Planet Change 24:27–39

Berger A (1978) Long-term variations of daily insolation and quaternary climatic changes. J Atmos Sci 35(12):2362–2367

Berger A, Loutre MF (2002) An exceptionally long interglacial ahead? Science 297:1287–1288

Berger A, Loutre MF (2003) Climate 400,000 years ago, a key to the future? In: Droxler A, Burckle L, Poore A (eds) Earth climate and orbital eccentricity: the marine isotope stage 11 question. Geophysical monograph 137. American Geophysical Union, Washington, pp 17–26

Berger A, Loutre MF, Mélice JL (2006) Equatorial insolation: from precession harmonics to eccentricity frequencies. Clim Past 2:131–136. doi:10.5194/cp-2-131-2006

Billups K, Scheinwald A (2014) Origin of millennial-scale climate signals in the subtropical North Atlantic. Paleoceanography 29:612–627. doi:10.1002/2014PA002641

Billups K, Rabideaux N, Stoffel J (2011) Suborbital-scale surface and deep water records in the subtropical North Atlantic: implications on thermohaline overturn. Quat Sci Rev 30:2976–2987. doi:10.1016/j.quascirev.2011.06.015

Bintanja R, van de Wal RSW (2008) North American ice-sheet dynamics and the onset of 100,000-year glacial cycles. Nature 454:869–872. doi:10.1038/nature07158

Bintanja R, van de Wal RSW, Oerlemans J (2005) Modelled atmospheric temperatures and global sea levels over the past million years. Nature 437:125–128. doi:10.1038/nature03975

Bosmans JHC, Drijfhout SS, Tuenter E, Hilgen FJ, Lourens LJ, Rohling EJ (2015) Precession and obliquity forcing of the

freshwater budget over the Mediterranean. Quat Sci Rev 123:16–30. doi:10.1016/j.quascirev.2015.06.008

Bounceur N, Crucifix M, Wilkinson RD (2015) Global sensitivity analysis of the climate–vegetation system to astronomical forcing: an emulator-based approach. Earth Syst Dyn 6:205–224. doi:10.5194/esd-6-205-2015

Bradshaw RHW, Webb T (1985) Relationships between contemporary pollen and vegetation data from Wisconsin and Michigan, USA. Ecology 66:721–737. doi:10.2307/1940533

Brovkin V, Ganapolski A, Svirezhev Y (1997) A continuous climate vegetation classification for use in climate-biosphere studies. Ecol Modell 101:251–261

Candy I, Mcclymont EL (2013) Interglacial intensity in the North Atlantic over the last 800000 years: Investigating the complexity of the mid-Brunhes event. J Quat Sci 28:343–348. doi:10.1002/jqs.2632

Candy I, Schreve DC, Sherriff J, Tye GJ (2014) Marine Isotope Stage 11: Palaeoclimates, palaeoenvironments and its role as an analogue for the current interglacial. Earth-Science Rev 128:18–51. doi:10.1016/j.earscirev.2013.09.006

Castro EB, González MAC, Tenorio MC, Bombín RE, Antón MG, Fuster MG, Manzaneque FG, Sáiz JCM, Juaristi CM, Pajares PR, Ollero HS (1997) Los bosques ibéricos: una Interpretación Geobotánica. Editorial Planeta, Barcelona, p 572

Chabaud L, Sánchez Goñi MF, Desprat S, Rossignol L (2014) Land-sea climatic variability in the eastern North Atlantic subtropical region over the last 14,200 years: atmospheric and oceanic processes at different timescales. Holocene 24:787–797. doi:10.1177/0959683614530439

Clark PU, Alley RB, Pollard D (1999) Northern Hemisphere ice sheet influences on global climate change. Science 286:1104–1111

Cramer W, Bondeau A, Woodward FI, Prentice IC, Betts RA, Brovkin V, Cox PM, Fisher V, Foley JA, Friend AD, Kucharik C, Lomas MR, Ramankutty N, Sitch S, Smith B, White A, Young-Molling C (2001) Global response of terrestrial ecosystem structure and function to CO_2 and climate change: results from six dynamic global vegetation models. Global Change Biol 7:357–373

de Vernal A, Hillaire-Marcel C (2008) Natural variability of Greenland climate, vegetation, and ice volume during the past million years. Science 320:1622–1625. doi:10.1126/science.1153929

de Beaulieu JL, Andrieu-Ponel V, Reille M, Grüger E, Tzedakis C, Svobodova H (2001) An attempt at correlation between the Velay pollen sequence and the Middle Pleistocene stratigraphy from central Europe. Quat Sci Rev 20:1593–1602. doi:10.1016/S0277-3791(01)00027-0

de Abreu L, Abrantes FF, Shackleton NJ, Tzedakis PC, McManus JF, Oppo DW, Hall MA (2005) Ocean climate variability in the eastern North Atlantic during interglacial marine isotope stage 11: a partial analogue to the Holocene? Paleoceanography 20:1–15. doi:10.1029/2004PA001091

Desprat S, Sánchez Goñi MF, Naughton F, Turon JL, Duprat J, Malaize B, Cortijo E, Peypouquet JP (2007) Climate variability of the last five isotopic interglacials: direct land-sea-ice correlation from the multiproxy analysis of North-Western Iberian margin deep-sea cores. Dev Quat Sci 7:375–386

Desprat S, Combourieu-Nebout N, Essallami L, Sicre MA, Dormoy I, Peyron O, Siani G, Bout Roumazeilles V, Turon JL (2013) Deglacial and holocene vegetation and climatic changes in the southern central Mediterranean from a direct land-sea correlation. Clim Past 9:767–787. doi:10.5194/cp-9-767-2013

Dickson AJ, Beer CJ, Dempsey C, Maslin MA, Bendle JA, McClymont EL, Pancost RD (2009) Oceanic forcing of the Marine Isotope Stage 11 interglacial. Nat Geosci 2:428–433. doi:10.1038/ngeo527

Droxler AW, Farrell JW (2000) Marine Isotope Stage 11 (MIS 11): new insights for a warm future. Glob Planet Change 24:1–5

Droxler AW, Poore RZ, Burckle LH (eds) (2003) Earth's climate and orbital eccentricity: the marine isotope stage 11 question. Geophysical Monograph Series. American Geophysical Union, Washington, D. C., p 240. ISBN:0-87590-996-5

Dutton A, Carlson AE, Long AJ, Milne GA, Clark PU, DeConto R, Horton BP, Rahmstorf S, Raymo ME (2015) Sea-level rise due to polar ice-sheet mass loss during past warm periods. Science 349:aaa4019. doi:10.1126/science.aaa4019

EPICA CM (2004) Eight glacial cycles from an Antarctic ice core. Nature 429:623–628

Expedition 339 Scientists (2013) Site U1385. In: Stow DAV, Hernández-Molina FJ, Alvarez Zarikian CA, the Expedition 339 Scientists (eds) Proceedings IODP 339. Integrated Ocean Drilling Program Management International, Inc., Tokyo. doi:10.2204/iodp.proc.339.103.201

Faegri K, Kaland PE, Krzywinski K (1989) Textbook of pollen analysis, Fourth edn. Wiley, Chichester, p 328

Ferretti P, Crowhurst SJ, Hall MA, Cacho I (2010) North Atlantic millennial-scale climate variability 910 to 790 ka and the role of the equatorial insolation forcing. Earth Planet Sci Lett 293:28–41. doi:10.1016/j.epsl.2010.02.016

Ferretti P, Crowhurst SJ, Naafs BDA, Barbante C (2015) The Marine Isotope Stage 19 in the mid-latitude North Atlantic Ocean: astronomical signature and intra-interglacial variability. Quat Sci Rev 108:95–110. doi:10.1016/j.quascirev.2014.10.024

Fiúza AFG (1984) Hidrologia e Dinâmica das Águas Costeiras de Portugal. Ph.D. Dissertation, University of Lisbon, p 294

Fletcher WJ, Sánchez Goñi MF (2008) Orbital- and sub-orbital-scale climate impacts on vegetation of the western Mediterranean basin over the last 48,000 year. Quat Res 70:451–464. doi:10.1016/j.yqres.2008.07.002

Ganopolski A, Winkelmann R, Schellnhuber HJ (2016) Critical insolation–CO_2 relation for diagnosing past and future glacial inception. Nature 529:200–203. doi:10.1038/nature16494

Giaccio B, Regattieri E, Zanchetta G, Nomade S, Renne PR, Sprain CJ, Drysdale RN, Tzedakis PC, Messina P, Scardia G, Sposato A, Bassinot F (2015) Duration and dynamics of the best orbital analogue to the present interglacial. Geology 43:603–606. doi:10.1130/G36677.1

Goosse H, Brovkin V, Fichefet T, Haarsma R, Huybrechts P, Jongma J, Mouchet A, Selten F, Barriat PY, Campin JM, Deleersnijder E, Driesschaert E, Goelzer H, Janssens I, Loutre MF, Maqueda MAM, Opsteegh T, Mathieu PP, Munhoven G, Petterson JE, Renssen H, Roche D, Schaeffer M, Tartinville B, Timmermann A, Weber SL (2010) Description of the earth system model of intermediate complexity LOVECLIM version 1.2. Geosci Model Dev 3:603–633

Gouveia C, Trigo RM, DaCamara CC, Libonati R, Pereira JMC (2008) The North Atlantic Oscillation and European vegetation dynamics. Int J Climatol 28:1835–1847

Helmke JP, Bauch HA, Röhl U, Kandiano ES (2008) Uniform climate development between the subtropical and subpolar Northeast Atlantic across marine isotope stage 11. Clim Past 4:181–190. doi:10.5194/cp-4-181-2008

Hernández-Almeida I, Sierro FJ, Cacho I, Flores JA (2012) Impact of suborbital climate changes in the North Atlantic on ice sheet dynamics at the Mid-Pleistocene Transition. Paleoceanography. doi:10.1029/2011PA002209

Heusser L, Balsam WL (1977) Pollen distribution in the northeast Pacific Ocean. Quat Res 7:45–62. doi:10.1016/0033-5894(77)90013-8

Hodell DA, Channell JET (2016) Mode transitions in Northern Hemisphere glaciation: co-evolution of millennial and orbital variability in Quaternary climate. Clim Past 12:1805–1828. doi:10.5194/cp-12-1805-2016

Hodell DA, Channeil JET, Curtis JH, Romero OE, Röhl U (2008) Onset of "Hudson Strait" Heinrich events in the eastern North Atlantic at the end of the middle Pleistocene transition (~ 640 ka)? Paleoceanography 23:1–16. doi:10.1029/2008PA001591

Hodell DA, Lourens L, Stow DV, Hernández-Molina J, Alvarez Zarikian C, Shackleton Site Project Members (2013) The "Shackleton Site" (IODP Site U1385) on the Iberian Margin. Proc Integr Ocean Drill Progr 16:13–19. doi:10.5194/sd-16-13-2013

Hodell D, Lourens L, Crowhurst S, Konijnendijk T, Tjallingii R, Jimenez-Espejo F, Skinner L, Tzedakis PC (2015) A reference time scale for Site U1385 (Shackleton Site) on the SW Iberian Margin. Glob Planet Change 1385:49–64. doi:10.1016/j.gloplacha.2015.07.002

IPCC (2013) Climate Change 2013: the physical science basis. Contribution of Working Group I to the Fifth Assessment Report of the Intergovernmental Panel on Climate Change. In: Stocker TF, Qin D, Plattner GK, Tignor M, Allen SK, Boschung J, Nauels A, Xia Y, Bex V, Midgley PM (eds) Cambridge University Press, Cambridge, p 1535. doi:10.1017/CBO9781107415324

Kandiano ES, Bauch HA, Fahl K, Helmke JP, Röhl U, Pérez-Folgado M, Cacho I (2012) The meridional temperature gradient in the eastern North Atlantic during MIS 11 and its link to the ocean–atmosphere system. Palaeogeogr Palaeoclimatol Palaeoecol 333–334:24–39. doi:10.1016/j.palaeo.2012.03.005

Lang N, Wolff EW (2011) Interglacial and glacial variability from the last 800 ka in marine, ice and terrestrial archives. Clim Past 7:361–380. doi:10.5194/cp-7-361-2011

Lionello P, Malanotte-Rizzoli P, Boscolo R, Alpert P, Artale V, Li L, Luterbacher J, May W, Trigo R, Tsimplis M, Ulbrich U, Xoplaki E (2006) The Mediterranean climate: an overview of the main characteristics and issues. Dev Earth Environ Sci 4:1–26. doi:10.1016/S1571-9197(06)80003-0

Lisiecki LE, Raymo ME (2005) A Pliocene–Pleistocene stack of 57 globally distributed benthic $\delta^{18}O$ records. Paleoceanography. doi:10.1029/2004PA001071

Loidi J, Biurrun I, Campos JA, Garcia-Mijangos I, Herrera M (2007) A survey of heath vegetation of the Iberian Peninsula and Northern Morocco: a biogeographical and bioclimatic approach. Phytocoenologia 37:341–370

Loutre MF, Berger AL (2003) Marine Isotope Stage 11 as an analogue for the present interglacial. Glob Planet Change 36:209–217. doi:10.1016/S0921-8181(02)00186-8

Lüthi D, Le Floch M, Bereiter B, Blunier T, Barnola JM, Siegenthaler U, Raynaud D, Jouzel J, Fischer H, Kawamura K, Stocker TF (2008) High-resolution carbon dioxide concentration record 650,000–800,000 years before present. Nature 453:379–382. doi:10.1038/nature06949

Magny M, Vannière B, Calo C, Millet L, Leroux A, Peyron O, Zanchetta G, La Mantia T, Tinner W (2011) Holocene hydrological changes in south-western Mediterranean as recorded by lake-level fluctuations at Lago Preola, a coastal lake in southern Sicily, Italy. Quat Sci Rev 30:2459–2475. doi:10.1016/j.quascirev.2011.05.018

Magny M, Combourieu-Nebout N, De Beaulieu JL, Bout-Roumazeilles V, Colombaroli D, Desprat S, Francke A, Joannin S, Ortu E, Peyron O, Revel M, Sadori L, Siani G, Sicre MA, Samartin S, Simonneau A, Tinner W, Vannière B, Wagner B, Zanchetta G, Anselmetti F, Brugiapaglia E, Chapron E, Debret M, Desmet M, Didier J, Essallami L, Galop D, Gilli A, Haas JN, Kallel N, Millet L, Stock A, Turon JL, Wirth S, Vannière B, Calo C, Millet L, Leroux A, Peyron O, Zanchetta G, La Mantia T, Tinner W (2013) North-south palaeohydrological contrasts in the central mediterranean during the Holocene: tentative synthesis and working hypotheses. Clim Past 9:2459–2475. doi:10.1016/j.quascirev.2011.05.018

Magri D (2012) Quaternary history of Cedrus in Southern Europe. Ann Di Bot 57–66. doi:10.4462/annbotrm-10022

Magri D, Tzedakis P (2000) Orbital signatures and long-term vegetation patterns in the Mediterranean. Quat Int 73–74:69–78. doi:10.1016/S1040-6182(00)00065-3

Margari V, Skinner LC, Hodell DA, Martrat B, Toucanne S, Grimalt JO, Gibbard PL, Lunkka JP, Tzedakis PC (2014) Land-ocean changes on orbital and millennial time scales and the penultimate glaciation. Geology 42:183–186. doi:10.1130/G35070.1

Masson-Delmotte V, Dreyfus G, Braconnot P, Johnsen S, Jouzel J, Kageyama M, Landais A, Loutre MF, Nouet J, Parrenin F, Raynaud D, Stenni B, Tuenter E (2006) Past temperature reconstructions from deep ice cores: relevance for future climate change. Clim Past 2:145–165. doi:10.5194/cp-2-145-2006

Masson-Delmotte V, Stenni B, Pol K, Braconnot P, Cattani O, Falourd S, Kageyama M, Jouzel J, Landais A, Minster B, Barnola JM, Chappellaz J, Krinner G, Johnsen S, Röthlisberger R, Hansen J, Mikolajewicz U, Otto-Bliesner B (2010) EPICA Dome C record of glacial and interglacial intensities. Quat Sci Rev 29:113–128. doi:10.1016/j.quascirev.2009.09.030

McManus J, Oppo D, Cullen J, Healey S (2003) Marine Isotope Stage 11 (MIS 11): Analog for Holocene and future climate? In: Droxler AW, Poore RZ, Burckle LH (eds) Earth's climate and orbital eccentricity: the marine isotope stage 11 question. American Geophysical Union, Washington D. C., pp 69–85

Melles M, Brigham-Grette J, Minyuk PS, Nowaczyk NR, Wennrich V, DeConto RM, Anderson PM, Andreev AA, Coletti A, Cook TL, Haltia-Hovi E, Kukkonen M, Lozhkin AV, Rosen P, Tarasov P, Vogel H, Wagner B (2012) 2.8 Million years of Arctic climate change from Lake El'gygytgyn. NE Russ Sci 337:315–320. doi:10.1126/science.1222135

Müller PJ, Kirst G, Ruhland G, Von Storch I, Rosell-Melé A (1998) Calibration of the alkenone paleotemperature index $U^{k'}_{37}$- based on core-tops from the eastern South Atlantic and the global ocean (60°N–60°S). Geochim Cosmochim Acta 62:1757–1772

Naafs BDA, Hefter J, Stein R (2013) Millennial-scale ice rafting events and Hudson Strait Heinrich (-like) Events during the late Pliocene and Pleistocene: a review. Quat Sci Rev 80:1–28. doi:10.1016/j.quascirev.2013.08.014

Naughton F, Sánchez Goñi MF, Desprat S, Turon JL, Duprat J, Malaizé B, Joli C, Cortijo E, Drago T, Freitas MC (2007) Present-day and past (last 25 000 years) marine pollen signal off western Iberia. Mar Micropaleontol 62:91–114. doi:10.1016/j.marmicro.2006.07.006

Naughton F, Sánchez Goñi MF, Rodrigues T, Salgueiro E, Costas S, Desprat S, Duprat J, Michel E, Rossignol L, Zaragosi S, Voelker AHL, Abrantes F (2016) Climate variability across the last deglaciation in NW Iberia and its margin. Quat Int 414:9–22. doi:10.1016/j.quaint.2015.08.073

Nieto-Lugilde D, Maguire KC, Blois JL, Williams JW, Fitzpatrick MC (2015) Close agreement between pollen-based and forest inventory-based models of vegetation turnover. Glob Ecol Biogeogr 24:905–916. doi:10.1111/geb.12300

Oliveira D, Desprat S, Rodrigues T, Naughton F, Hodell D, Trigo R, Rufino M, Lopes C, Abrantes F, Sánchez Goñi MF (2016) The complexity of millennial-scale variability in southwestern Europe during MIS 11. Quat Res. doi:10.1016/j.yqres.2016.09.002

Oliveira D, Sánchez Goñi MF, Naughton F, Polanco-Martínez JM, Jimenez-Espejo FJ, Grimalt JO, Martrat B, Voelker AHL, Trigo R, Hodell D, Abrantes F, Desprat S (2017) Unexpected weak seasonal climate in the western Mediterranean region during MIS 31, a high-insolation forced interglacial. Quat Sci Rev 161:1–17. doi:10.1016/j.quascirev.2017.02.013

Pailler D, Bard E (2002) High frequency palaeoceanographic changes during the past 140 000 year recorded by the organic

matter in sediments of the Iberian Margin. Palaeogeogr Palaeoclimatol Palaeoecol 81:431–452
Palumbo E, Flores J-A, Perugia C, Petrillo Z, Voelker AHL, Amore FO (2013) Millennial scale coccolithophore paleoproductivity and surface water changes between 445 and 360 ka (Marine Isotope Stages 12/11) in the Northeast Atlantic. Palaeogeogr Palaeoclimatol Palaeoecol 383–384:27–41. doi:10.1016/j.palaeo.2013.04.024
Past Interglacials Working Group of PAGES (2016) Interglacials of the last 800,000 years. Rev Geophys. doi:10.1002/2015RG000482
Peinado Lorca M, Martinez-Parras JM (1987) Castilla-La Mancha. In: Peinado Lorca M, Rivas-Martinez S (eds) La vegetación de España. Universidad de Alcala de Henares, Alcala de Henares, pp 163–196
Peliz A, Dubert J, Santos AMP, Oliveira PB, Le Cann B (2005) Winter upper ocean circulation in the Western Iberian basin—fronts, eddies and poleward flows: an overview. Deep Res Part I Oceanogr Res Pap 52:621–646. doi:10.1016/j.dsr.2004.11.005
Pol K, Masson-Delmotte V, Johnsen S, Bigler M, Cattani O, Durand G, Falourd S, Jouzel J, Minster B, Parrenin F (2010) New MIS 19 EPICA Dome C high resolution deuterium data: Hints for a problematic preservation of climate variability at sub-millennial scale in the "oldest ice". Earth Planet Sci Lett 298:95–103. doi:10.1016/j.epsl.2010.07.030
Pol K, Debret M, Masson-Delmotte V, Capron E, Cattani O, Dreyfus G, Falourd S, Johnsen S, Jouzel J, Landais A, Minster B, Stenni B (2011) Links between MIS 11 millennial to sub-millennial climate variability and long term trends as revealed by new high resolution EPICA Dome C deuterium data - A comparison with the Holocene. Clim Past 7:437–450. doi:10.5194/cp-7-437-2011
Polunin O, Walters M (1985) A Guide to the vegetation of Britain and Europe. Oxford University Press, New York, p 238
Prahl FG, Wakeham SG (1987) Calibration of unsaturation patterns in long-chain ketone compositions for palaeotemperature assessment. Nature 330:367–369. doi:10.1038/330367a0
Prentice IC, Berglund BE, Olsson T (1987) Quantitative forest composition sensing characteristics of pollen samples from Swedish lakes. Boreas 16:43–54
Quezel P (2002) Réflexions sur l'évolution de la flore et de la végétation au Maghreb méditerranéen. Ibis, Paris
Raymo ME, Mitrovica JX (2012) Collapse of polar ice sheets during the stage 11 interglacial. Nature 483:453–456. doi:10.1038/nature10891
Raynaud D, Barnola J-M, Souchez R, Lorrain R, Petit JR, Duval P, Lipenkov VY (2005) Palaeoclimatology: the record for marine isotopic stage 11. Nature 436:39–40. doi:10.1038/43639b
Reille M, Beaulieu J-L, Svobodova H, Andrieu-Ponel V, Goeury C (2000) Pollen analytical biostratigraphy of the last five climatic cycles from a long continental sequence from the Velay region (Massif Central, France). J Quat Sci 15:665–685
Reimer PJ, Bard E, Bayliss A, Beck JW, Blackwell PG, Ramsey CB, Buck CE, Cheng H, Edwards RL, Friedrich M, Grootes PM, Guilderson TP, Haflidason H, Hajdas I, Hattté C, Heaton TJ, Hoffmann DL, Hogg AG, Hughen KA, Kaiser KF, Kromer B, Manning SW, Niu M, Reimer RW, Richards DA, Scott M, Southon JR, Staff RA, Turney CSM, van der Plicht J (2013) IntCal13 and Marine13 radiocarbon age calibration curves 0–50,000 years cal BP. Radiocarbon 55:1869–1887
Renssen H, Seppa H, Heiri O, Roche DM, Goosse H, Fichefet T (2009) The spatial and temporal complexity of the Holocene thermal maximum. Nat Geosci 2:411–414
Reyes AV, Carlson AE, Beard BL, Hatfield RG, Stoner JS, Winsor K, Welke B, Ullman DJ (2014) South Greenland ice-sheet collapse during Marine Isotope Stage 11. Nature 510:525–528. doi:10.1038/nature13456
Rind D (1998) Latitudinal temperature gradients and climate change. J Geophys Res 103:5943–5971
Roberts DL, Karkanas P, Jacobs Z, Marean CW, Roberts RG (2012) Melting ice sheets 400,000 year ago raised sea level by 13 m: Past analogue for future trends. Earth Planet Sci Lett 357–358:226–237. doi:10.1016/j.epsl.2012.09.006
Rodrigues T, Grimalt JO, Abrantes FG, Flores JA, Lebreiro S (2009) Holocene interdependences of changes in sea surface temperature, productivity, and fluvial inputs in the Iberian continental shelf (Tagus mud patch). Geochemistry Geophys Geosystems 10:1–17. doi:10.1029/2008GC002367
Rohling EJ, Braun K, Grant K, Kucera M, Roberts AP, Siddall M, Trommer G (2010) Comparison between Holocene and Marine Isotope Stage-11 sea-level histories. Earth Planet Sci Lett 291:97–105. doi:10.1016/j.epsl.2009.12.054
Ruddiman WF (2005) Cold climate during the closest stage 11 analog to recent millennia. Quat Sci Rev 24:1111–1121
Ruddiman WF (2007) The early anthropogenic hypothesis: challenges and responses. Rev Geophys 45:1–37
Ruddiman WF, McIntyre A (1984) Ice-age thermal response and climatic role of the surface Atlantic Ocean, 40°N to 63°N. Geol Soc Am Bull 95:381–396
Salgueiro E, Naughton F, Voelker AHL, de Abreu L, Alberto A, Rossignol L, Duprat J, Magalhães VH, Vaqueiro S, Turon JL, Abrantes F (2014) Past circulation along the western Iberian margin: a time slice vision from the Last Glacial to the Holocene. Quat Sci Rev 106:316–329. doi:10.1016/j.quascirev.2014.09.001
Sánchez Goñi MF, Landais A, Fletcher WJ, Naughton F, Desprat S, Duprat J (2008) Contrasting impacts of Dansgaard-Oeschger events over a western European latitudinal transect modulated by orbital parameters. Quat Sci Rev 27:1136–1151. doi:10.1016/j.quascirev.2008.03.003
Sánchez Goñi MF, Rodrigues T, Hodell DA, Polanco-Martínez JM, Alonso-García M, Hernández-Almeida I, Desprat S, Ferretti P (2016) Tropically-driven climate shifts in southwestern Europe during MIS 19, a low eccentricity interglacial. Earth Planet Sci Lett 448:81–93. doi:10.1016/j.epsl.2016.05.018
Shackleton NJ, Hall MA, Vincent E (2000) Phase relationships between millennial-scale events 64,000–24,000 years ago. Paleoceanography 15:565–569. doi:10.1029/2000PA000513
Skinner LC, Shackleton NJ (2005) An Atlantic lead over Pacific deep-water change across Termination I: implications for the application of the marine isotope stage stratigraphy. Quat Sci Rev 24:571–580. doi:10.1016/j.quascirev.2004.11.008
Sousa PM, Trigo RM, Aizpurua P, Nieto R, Gimeno L, Garcia-Herrera R (2011) Trends and extremes of drought indices throughout the 20th century in the Mediterranean. Nat Hazards Earth Syst Sci 11:33–51. doi:10.5194/nhess-11-33-2011
Spratt RM, Lisiecki LE (2016) A Late Pleistocene sea level stack. Clim Past 12:1079–1092. doi:10.5194/cp-12-1079-2016
Stuiver M, Reimer PJ (1993) Extended ^{14}C database and revised CALIB radiocarbon calibration program. Radiocarbon 35:215–230
Trigo RM, Pozo-Vazquez D, Osborn TJ, Castro-Díez Y, Gamiz-Fortis S, Esteban-Parra MJ (2004) North Atlantic oscillation influence on precipitation, river flow and water resources in the Iberian peninsula. Int J Climatol 24:925–944. doi:10.1002/joc.1048
Trigo RM, Valente MA, Trigo IF, Miranda PMA, Ramos AM, Paredes D, García-Herrera R (2008) The impact of North Atlantic wind and cyclone trends on european precipitation and significant wave height in the Atlantic. Ann N Y Acad Sci 1146:212–234. doi:10.1196/annals.1446.014
Tzedakis PC (2007) Seven ambiguities in the Mediterranean palaeoenvironmental narrative. Quat Sci Rev 26:2042–2066. doi:10.1016/j.quascirev.2007.03.014

Tzedakis PC (2010) The MIS 11–MIS 1 analogy, southern European vegetation, atmospheric methane and the "early anthropogenic hypothesis. Clim Past 6:131–144. doi:10.5194/cp-6-131-2010

Tzedakis PC, Hooghiemstra H, Pälike H (2006) The last 1.35 million years at Tenaghi Philippon: revised chronostratigraphy and long-term vegetation trends. Quat Sci Rev 25:3416–3430. doi:10.1016/j.quascirev.2006.09.002

Tzedakis PC, Raynaud D, McManus JF, Berger A, Brovkin V, Kiefer T (2009a) Interglacial diversity. Nat Geosci 2:751–755. doi:10.1038/ngeo660

Tzedakis PC, Pälike H, Roucoux KH, de Abreu L (2009b) Atmospheric methane, southern European vegetation and low-mid latitude links on orbital and millennial timescales. Earth Planet Sci Lett 277:307–317. doi:10.1016/j.epsl.2008.10.027

Tzedakis PC, Channell JET, Hodell DA, Kleiven HF, Skinner LC (2012) Determining the natural length of the current interglacial. Nat Geosci 5:138–141. doi:10.1038/ngeo1358

Tzedakis PC, Crucifix M, Mitsui T, Wolff EW (2017) A simple rule to determine which insolation cycles lead to interglacials. Nature 542:427–432. doi:10.1038/nature21364

van der Wiel AM, Wijmstra TA (1987) Palynology of 112.8–197.8 m interval of the core Tenaghi Philippon III, Middle Pleistocene of Macedonia. Rev Palaeobot Palynol 52:89–117

Villanueva J, Pelejero C, Grimalt JO (1997) Clean-up procedures for the unbiased estimation of C_{37} alkenone sea surface temperatures and terrigenous n-alkane inputs in paleoceanography. J Chromatogr A 757:145–151. doi:10.1016/S0021-9673(96)00669-3

Weirauch D, Billups K, Martin P (2008) Evolution of millennial-scale climate variability during the mid-Pleistocene. Paleoceanography 23:PA3216. doi:10.1029/2007PA001584

Williams JW, Jackson ST (2003) Palynological and AVHRR observations of modern vegetational gradients in eastern North America. The Holocene 13:485–497. doi:10.1191/0959683603hl613rp

Yin QZ, Berger A (2010) Insolation and CO_2 contribution to the interglacial climate before and after the mid-brunhes event. Nat Geosci 3(4):243–246

Yin QZ, Berger A (2012) Individual contribution of insolation and CO_2 to the interglacial climates of the past 800,000 years. Clim Dyn 38:709–724. doi:10.1007/s00382-011-1013-5

Yin Q, Berger A (2015) Interglacial analogues of the Holocene and its natural near future. Quat Sci Rev 120:28–46. doi:10.1016/j.quascirev.2015.04.008p